Supporting Information

Unraveling the Ignition Chemistry of Singly Levitated Aluminum Iodate Hexahydrate (AIH) Particles

Grace L. Rizzo,[1] Souvick Biswas,[1] Michelle L. Pantoya,[*2] Ralf I. Kaiser[*1]

[1]Department of Chemistry, University of Hawai'i at Manoa, Honolulu, HI 96822, USA

[2] Department of Mechanical Engineering, Texas Tech University, Lubbock, TX 79409-1021, USA

*E-mail: ralfk@hawaii.edu

*E-mail: michelle.pantoya@ttu.edu

Calibration Methods:

The wavelength-dependent sensitivity of the spectrometer system along with the optical fiber was calibrated using a calibrated light source (Hamamatsu High Power UV-Vis Fiber Light Source; 200 – 1600 nm). While in real time scope mode, the collection optics (optical fiber, Ocean Insight model: OCF-109248) are connected to the calibrated light source. The integration time (6 ms) and averaging levels (Average: 5) are adjusted to maximize the light output of the source. Once adjusted, the light is then blocked to obtain a dark (background) spectrum (Figure S30a). After the dark spectrum is collected, the light source is then unblocked, and the sensitivity calibration curve is captured. The resultant sensitivity curve is depicted in Figure S30b, which was then used for spectral analysis.

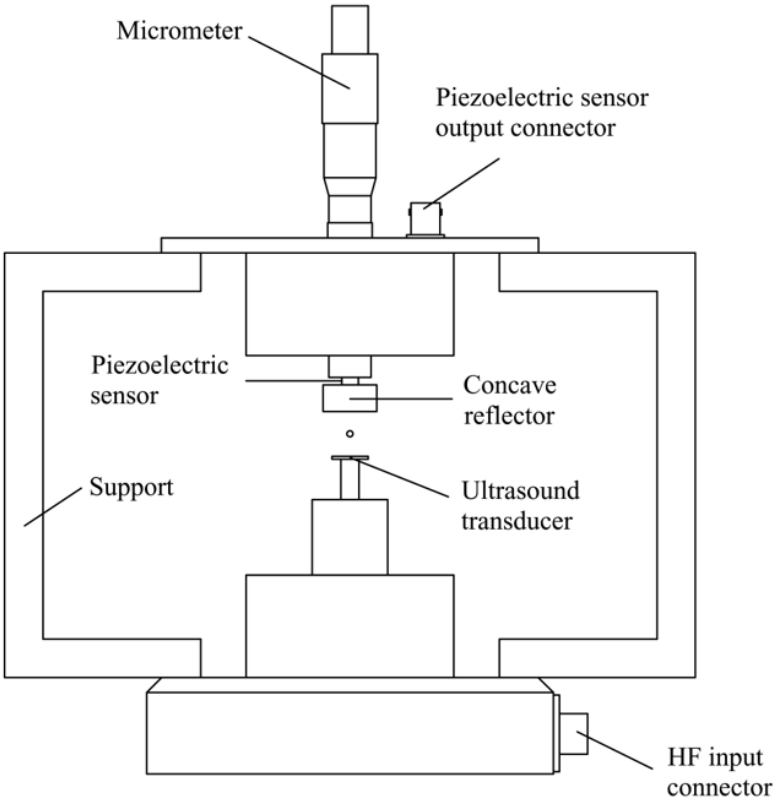

Figure S1. A schematic diagram of the levitator. Ultrasonic sound waves are generated by the piezoelectric transducer. A standing wave is generated due to multiple reflections between the transducer and the concave reflector. The micrometer displayed allows the distance between the transducer plate and the reflector to be adjusted. The pressure amplitude of the standing wave is monitored by connecting the output of the piezoelectric sensor via connector to an oscilloscope. The RF power to the transducer is input via the HF connector [1].

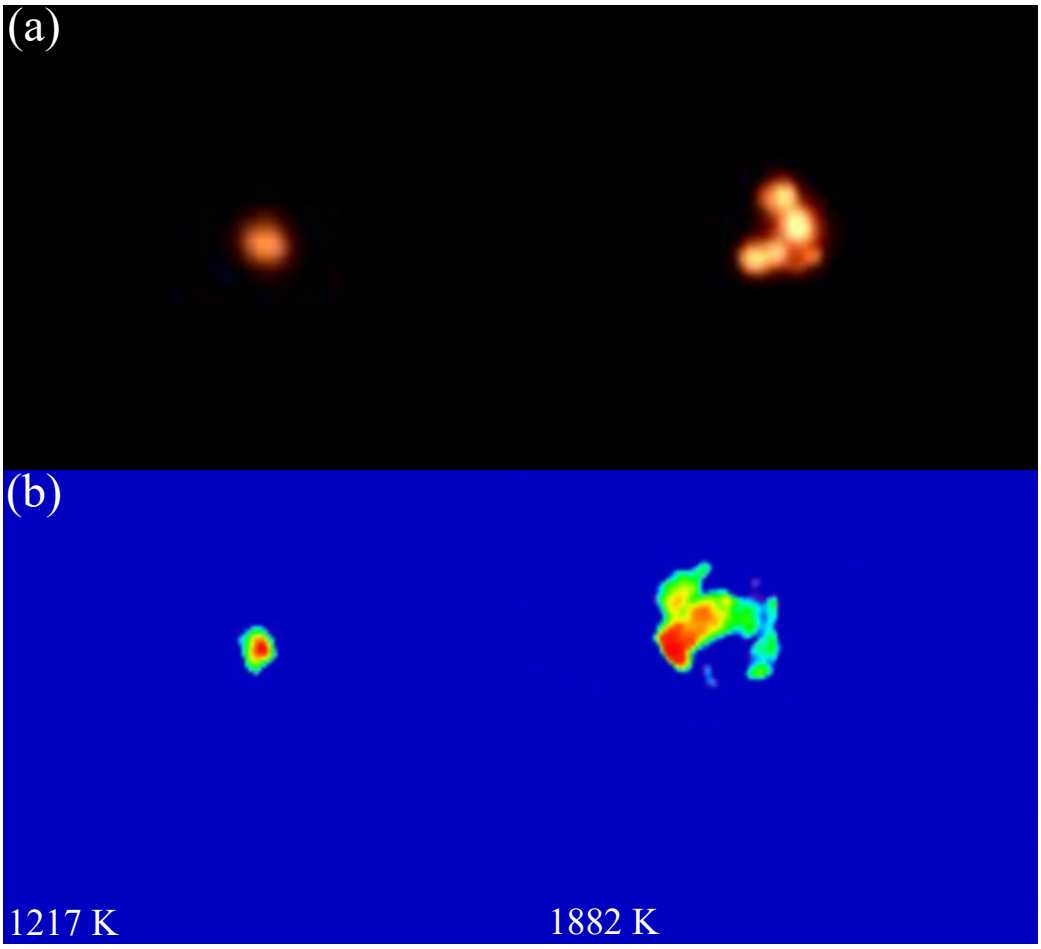

Figure S2. Optical and IR camera images taken during the levitation of AlH in 10% O_2 and 90% Ar. (a) represents the optical images taken during ignition. The image on the left at the beginning of the ignition and the right is point of the ignition where it is most intense. (b) represents the respective IR camera images to the images shown in (a). The respective temperatures are shown at the bottom of (b).

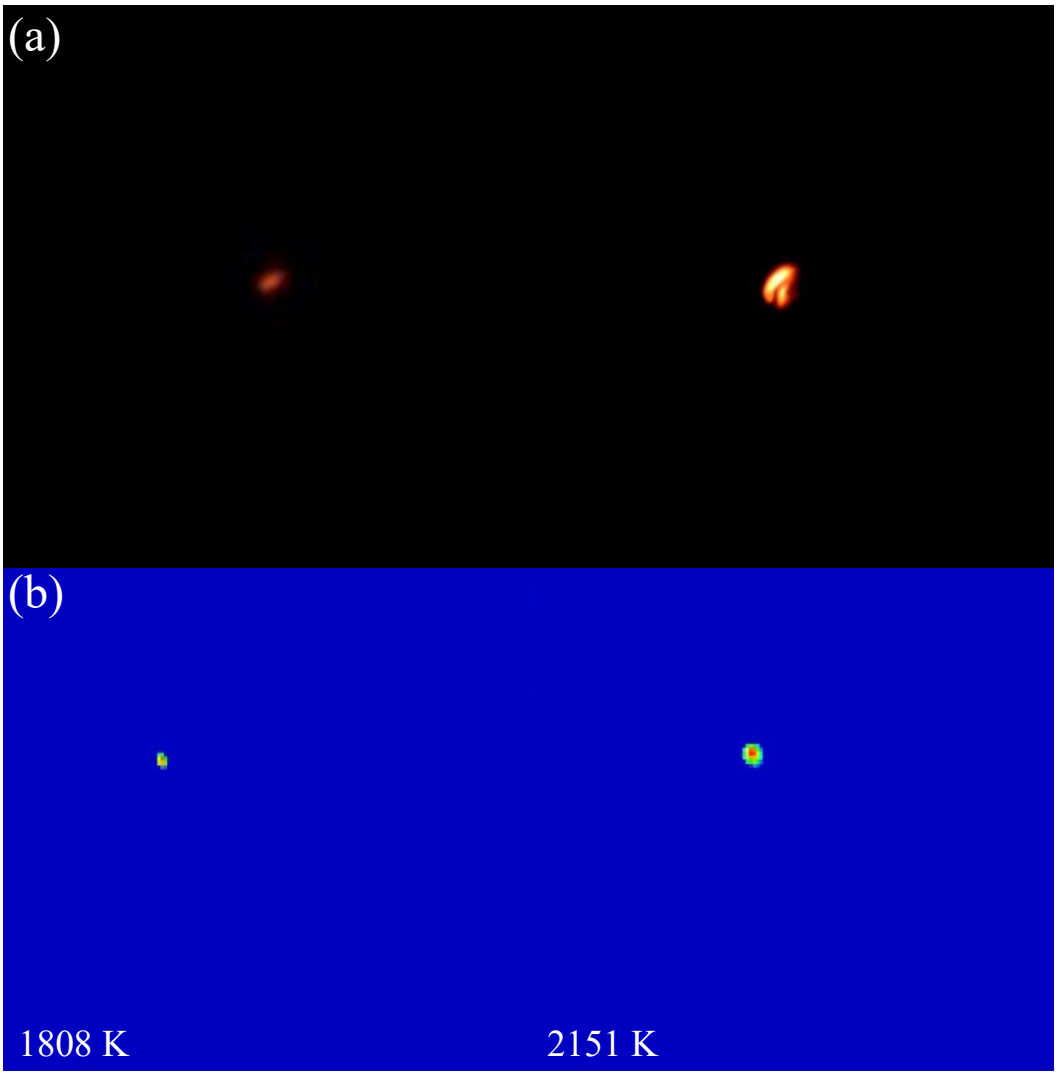

Figure S3. Optical and IR camera images taken during the levitation of AlH in 30% O_2 and 70% Ar. (a) represents the optical images taken during ignition. The image on the left at the beginning of the ignition and the right is point of the ignition where it is most intense. (b) represents the respective IR camera images to the images shown in (a). The respective temperatures are shown at the bottom of (b).

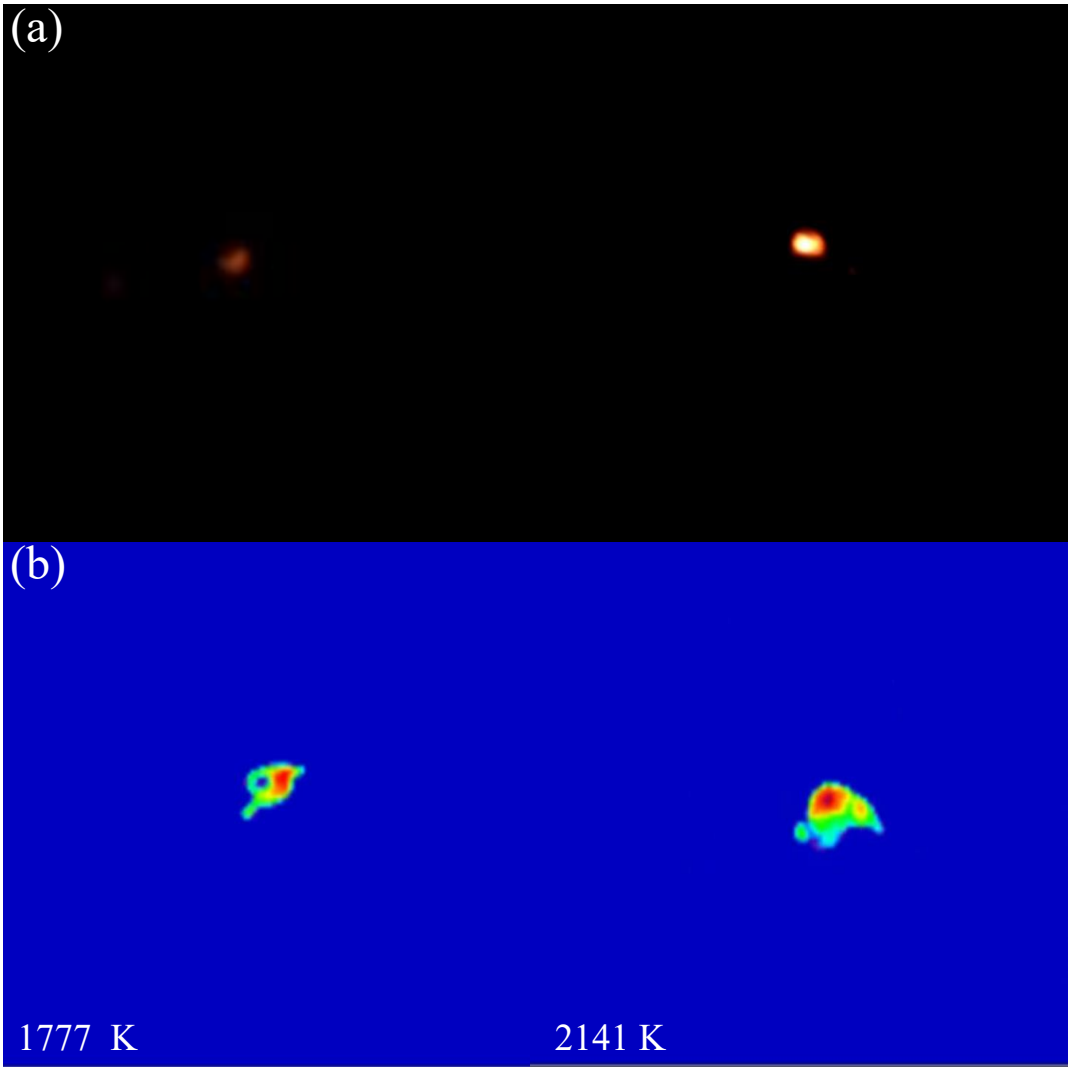

Figure S4. Optical and IR camera images taken during the levitation of AlH in 40% O_2 and 60% Ar. (a) represents the optical images taken during ignition. The image on the left at the beginning of the ignition and the right is point of the ignition where it is most intense. (b) represents the respective IR camera images to the images shown in (a). The respective temperatures are shown at the bottom of (b).

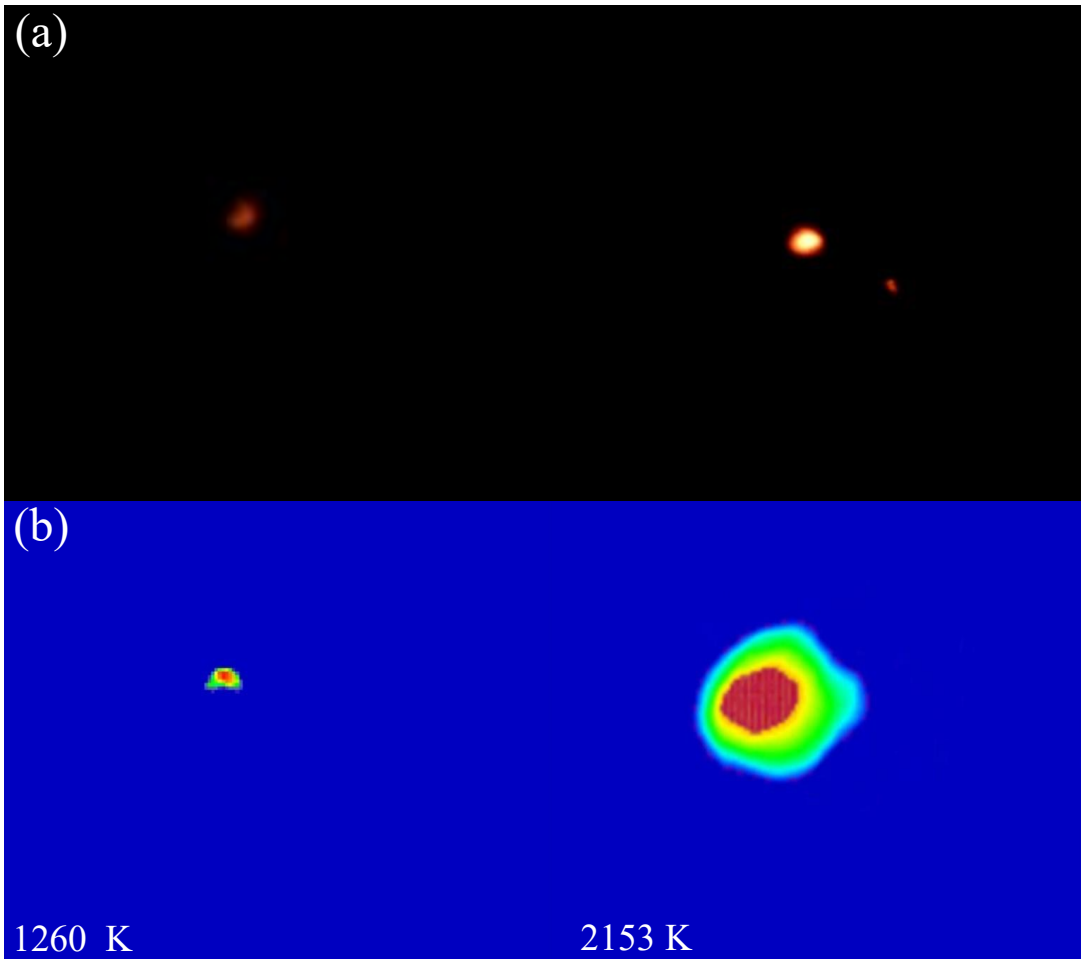

Figure S5. Optical and IR camera images taken during the levitation of AlH in 50% O_2 and 50% Ar. (a) represents the optical images taken during ignition. The image on the left at the beginning of the ignition and the right is point of the ignition where it is most intense. (b) represents the respective IR camera images to the images shown in (a). The respective temperatures are shown at the bottom of (b).

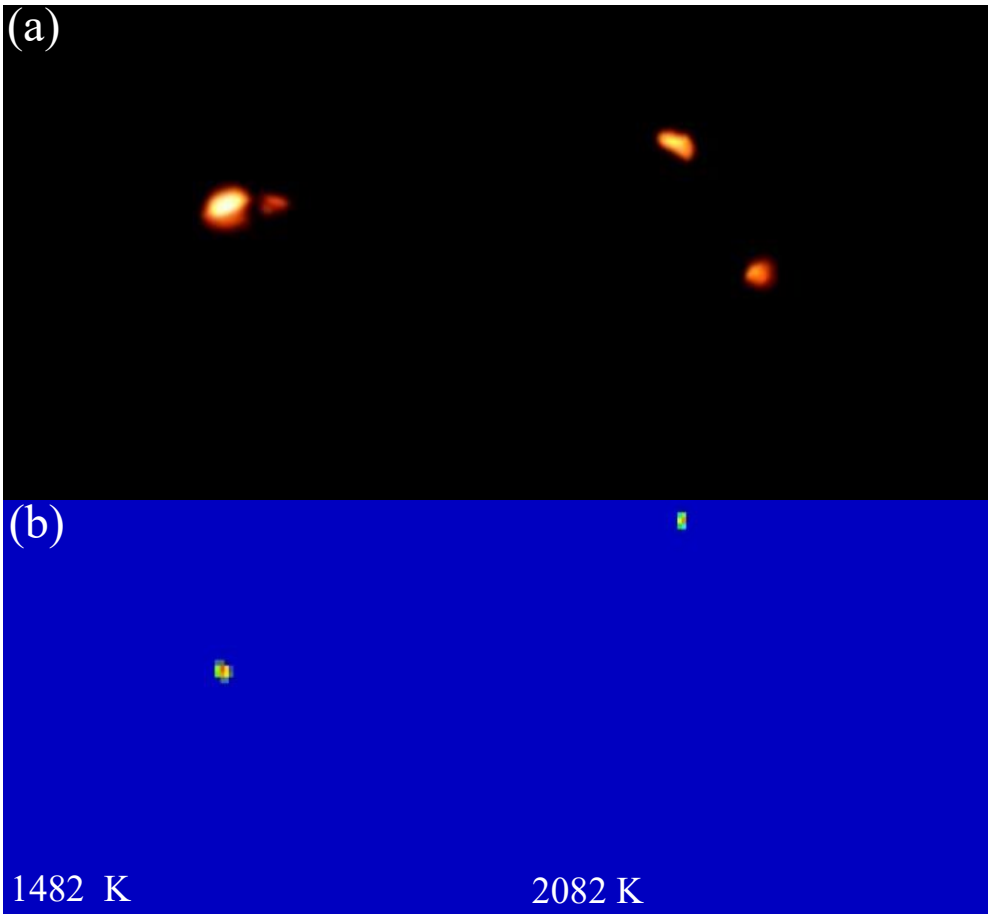

Figure S6. Optical and IR camera images taken during the levitation of AlH in 60% O_2 and 40% Ar. (a) represents the optical images taken during ignition. The image on the left at the beginning of the ignition and the right is point of the ignition where it is most intense. (b) represents the respective IR camera images to the images shown in (a). The respective temperatures are shown at the bottom of (b).

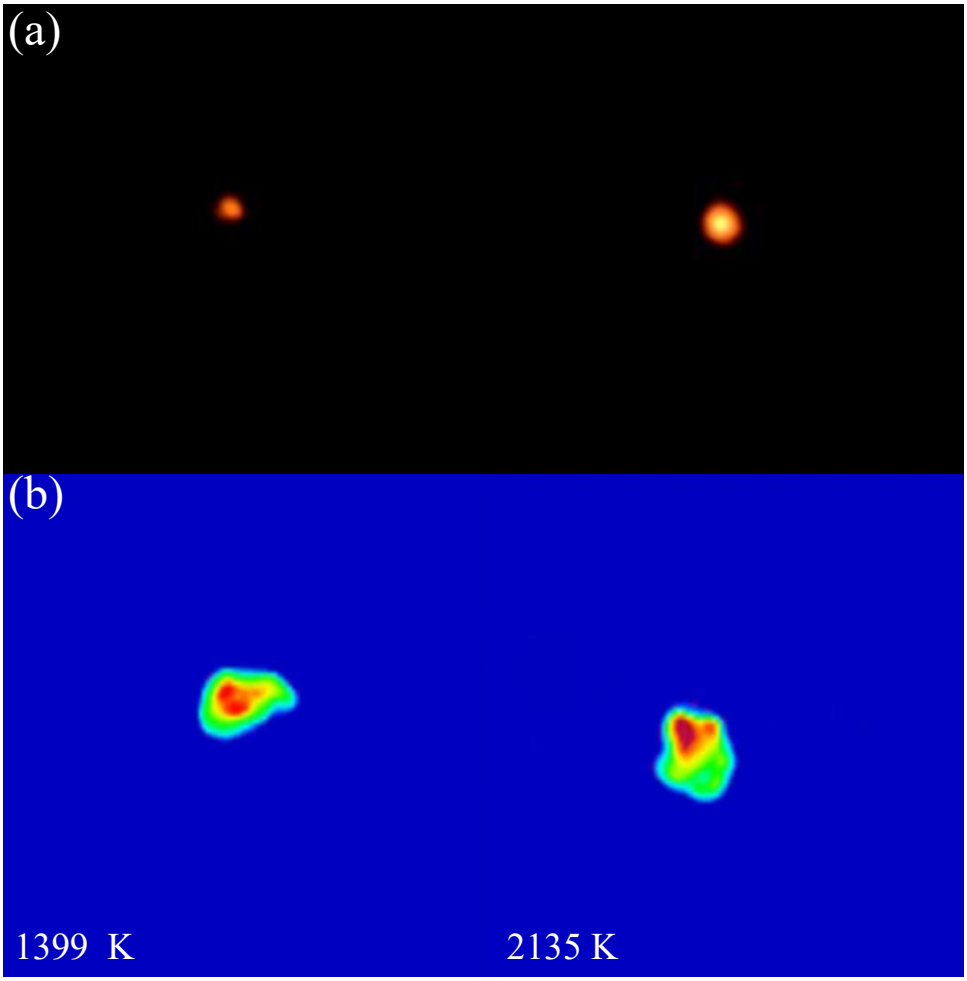

Figure S7. Optical and IR camera images taken during the levitation of AIH in 70% O_2 and 30% Ar. (a) represents the optical images taken during ignition. The image on the left at the beginning of the ignition and the right is point of the ignition where it is most intense. (b) represents the respective IR camera images to the images shown in (a). The respective temperatures are shown at the bottom of (b).

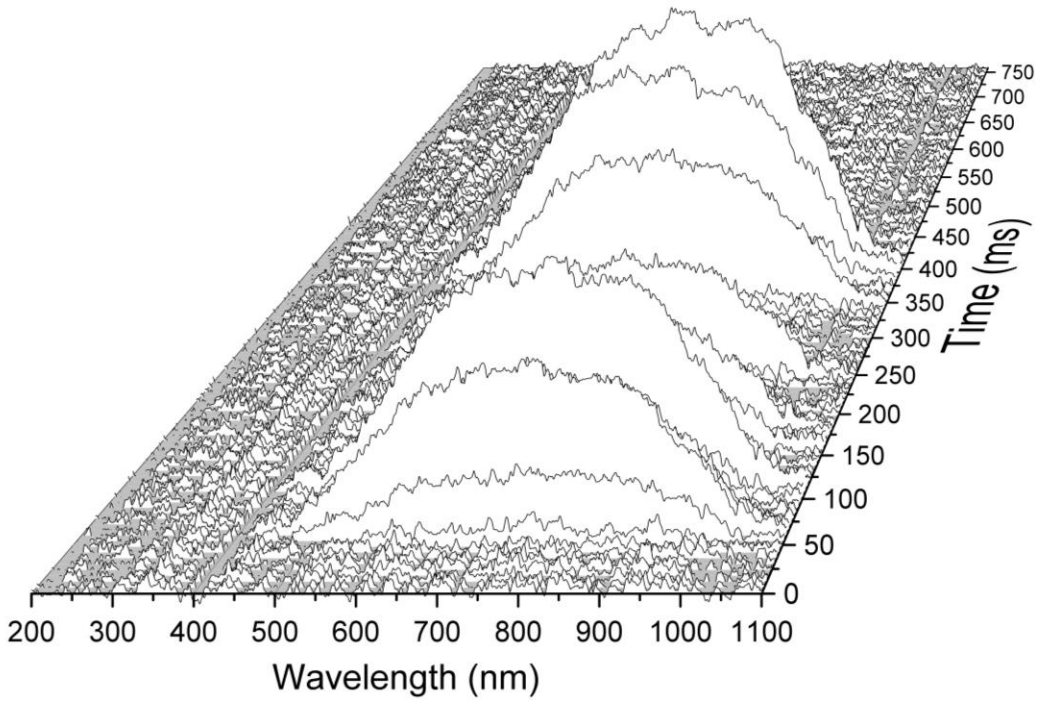

Figure S8. 3D plot of the AIH emission spectra when levitated in 10% O_2 and 90% Ar.

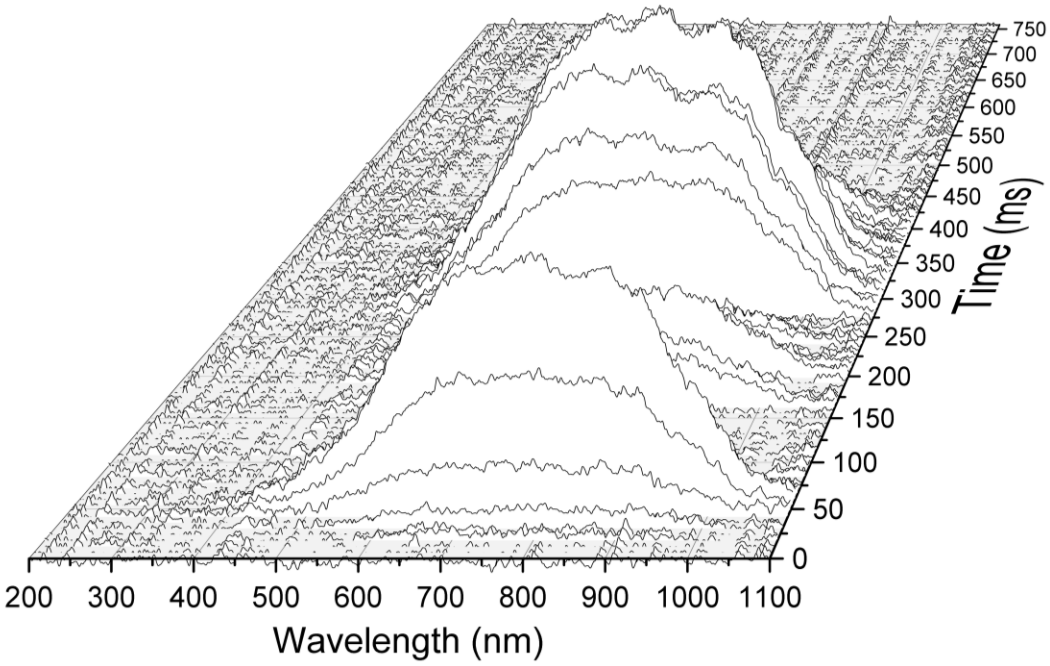

Figure S9. 3D plot of the AIH emission spectra when levitated in 30% O_2 and 70% Ar.

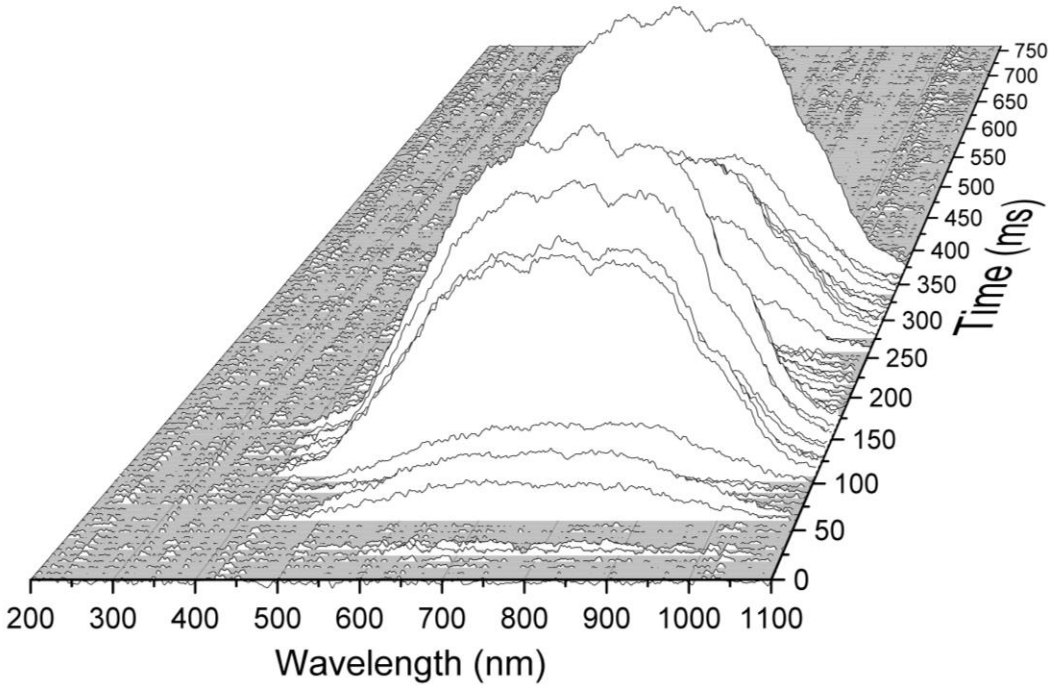

Figure S10. 3D plot of the AIH emission spectra when levitated in 40% O_2 and 60% Ar.

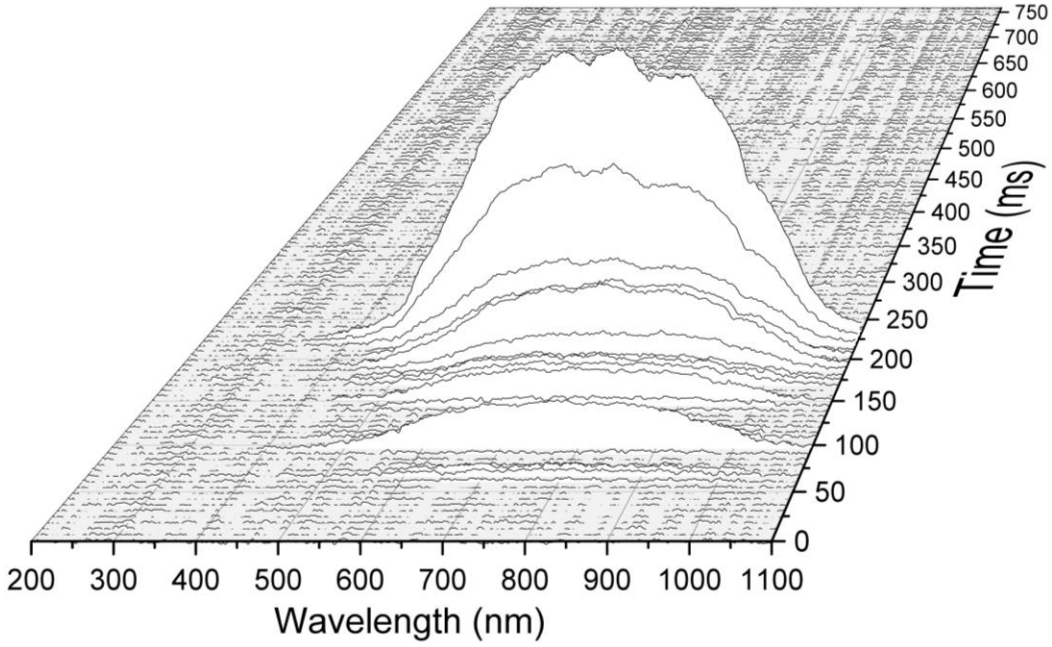

Figure S11. 3D plot of the AIH emission spectra when levitated in 50% O_2 and 50% Ar.

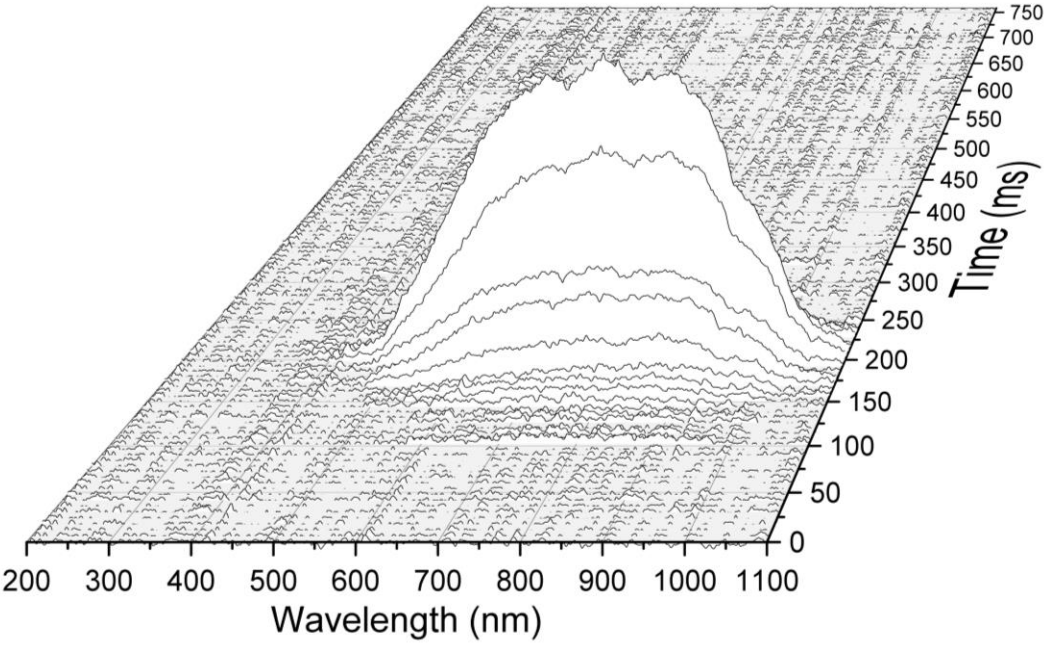

Figure S12. 3D plot of the AIH emission spectra when levitated in 60% O_2 and 40% Ar.

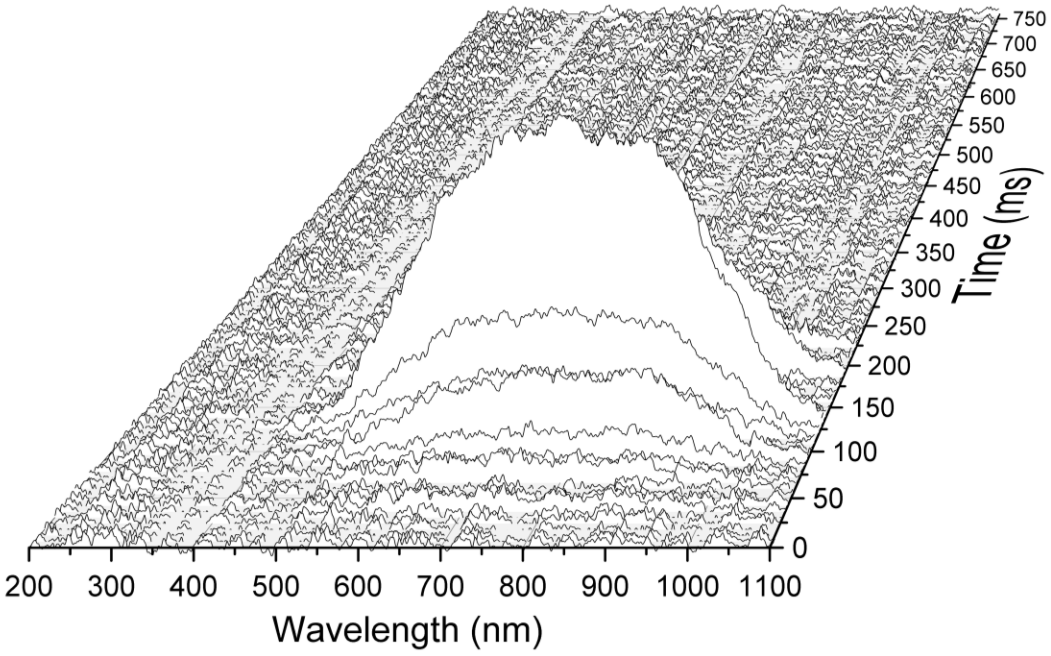

Figure S13. 3D plot of the AIH emission spectra when levitated in 70% O_2 and 30% Ar.

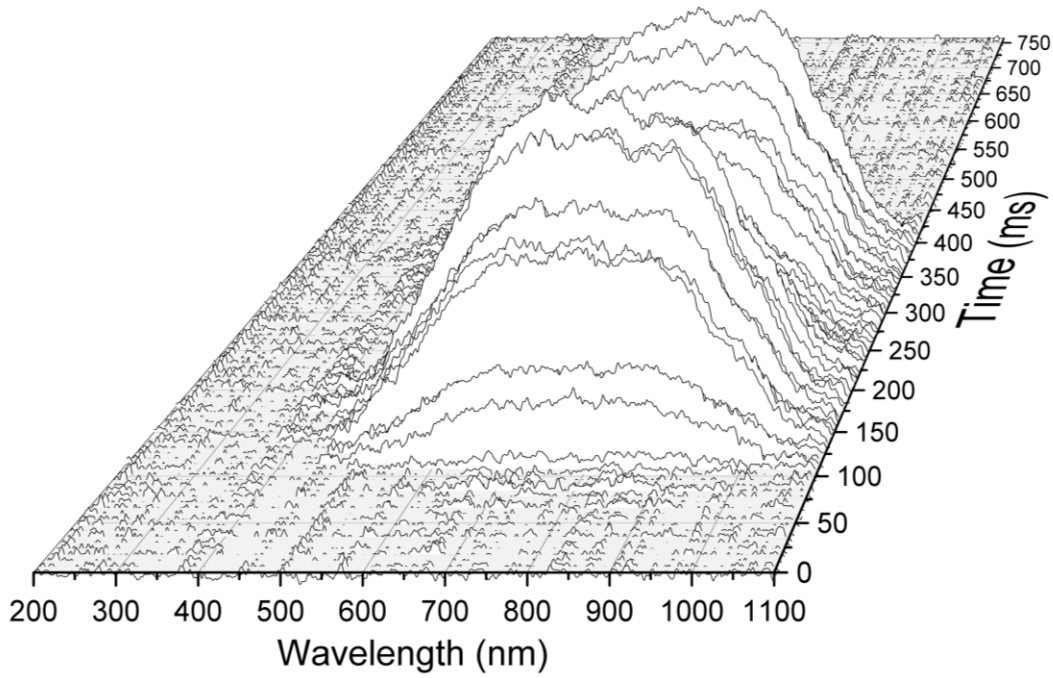

Figure S14. 3D plot of the AIH emission spectra when levitated in 80% O_2 and 20% Ar.

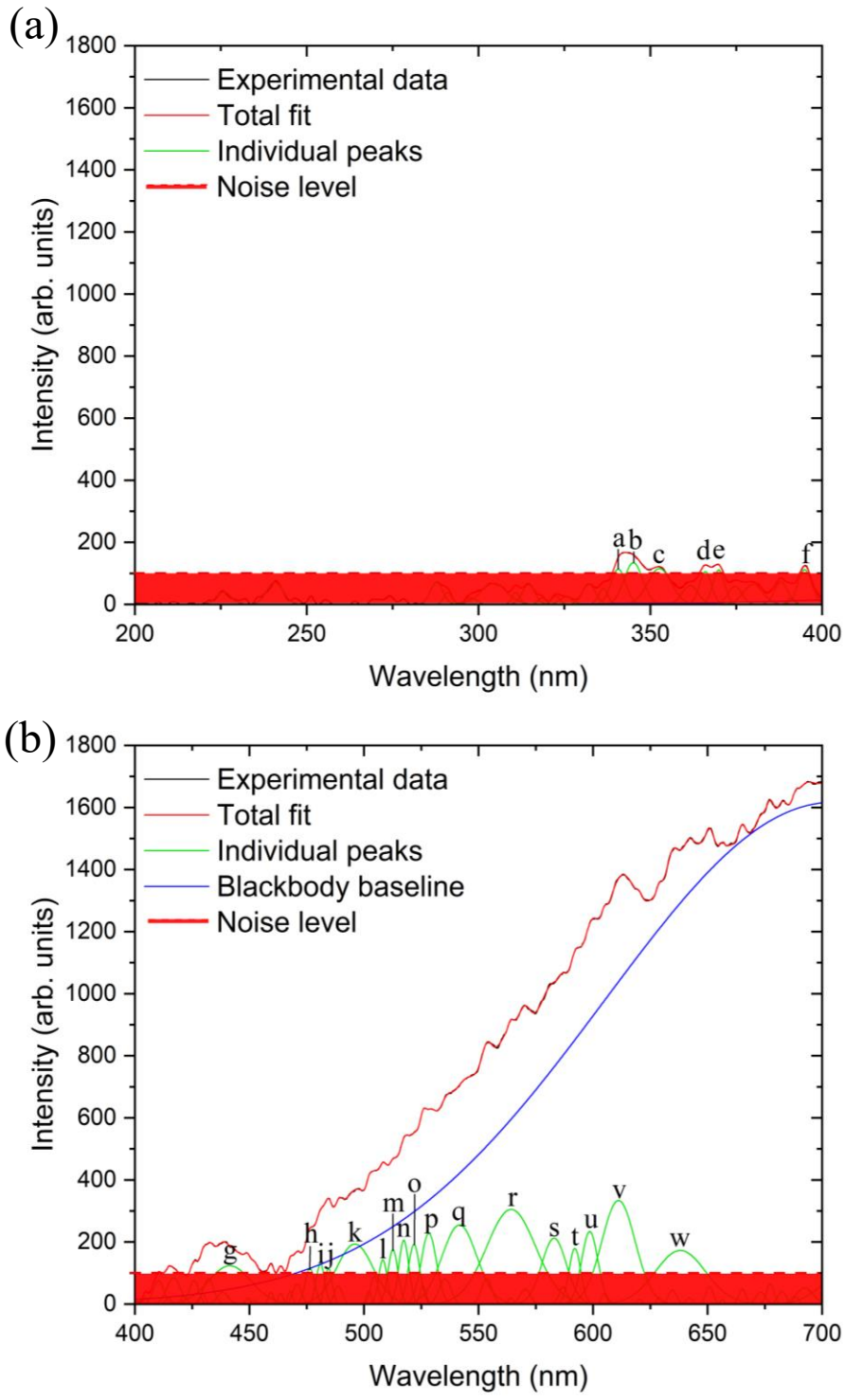

Figure S15. Deconvoluted UV-Vis emission spectrum of the levitated AIH particle in 10% O_2 and 90% Ar. (a) represents the wavelength region from 200 to 400 nm and (b) represents the wavelength region from 400 to 700 nm. See Table S1 for peak assignments.

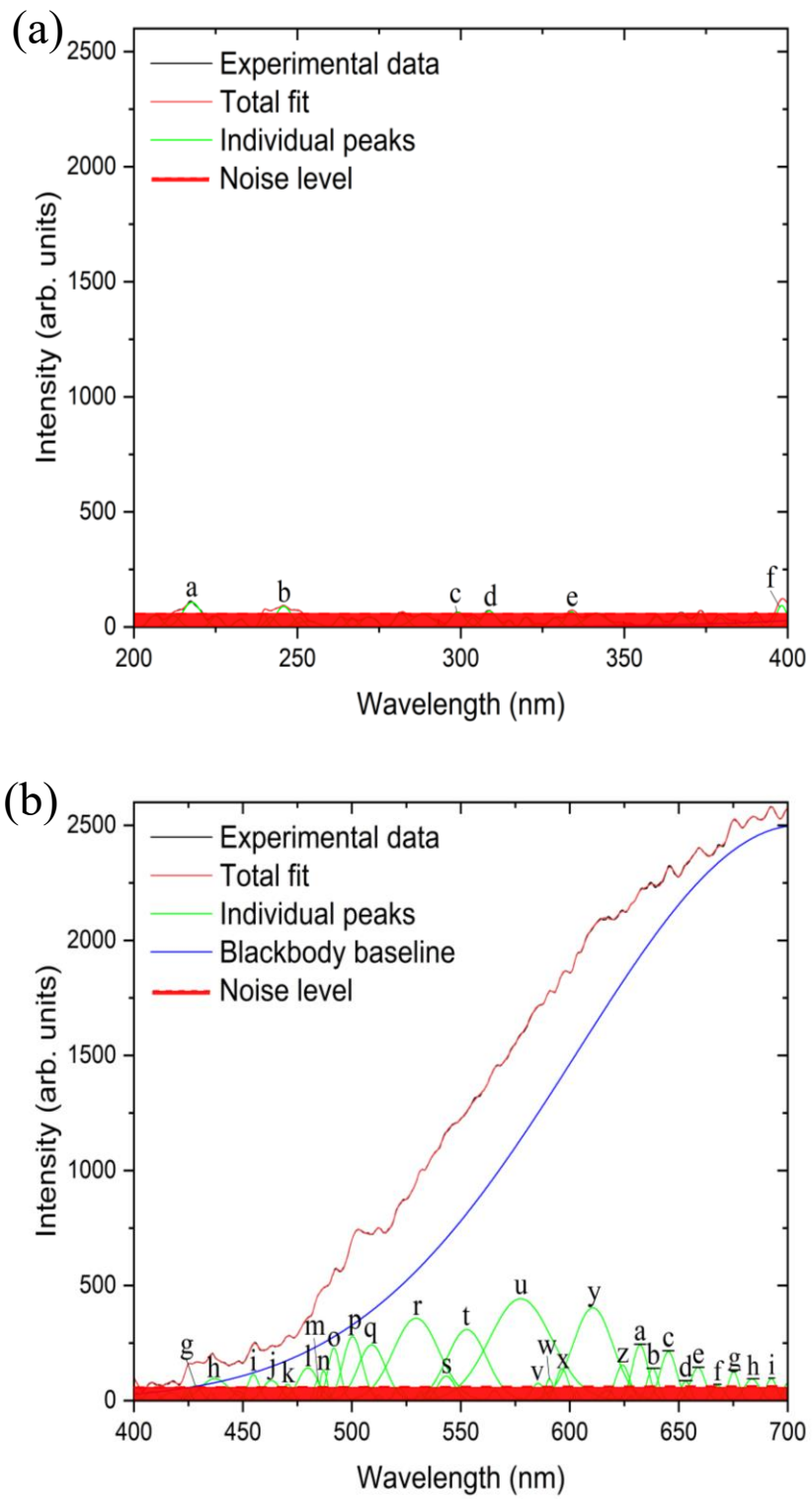

Figure S16. Deconvoluted UV-Vis emission spectrum of the levitated AIH particle in 30% O_2 and 70% Ar. (a) represents the wavelength region from 200 to 400 nm and (b) represents the wavelength region from 400 to 700 nm. See Table S2 for peak assignments.

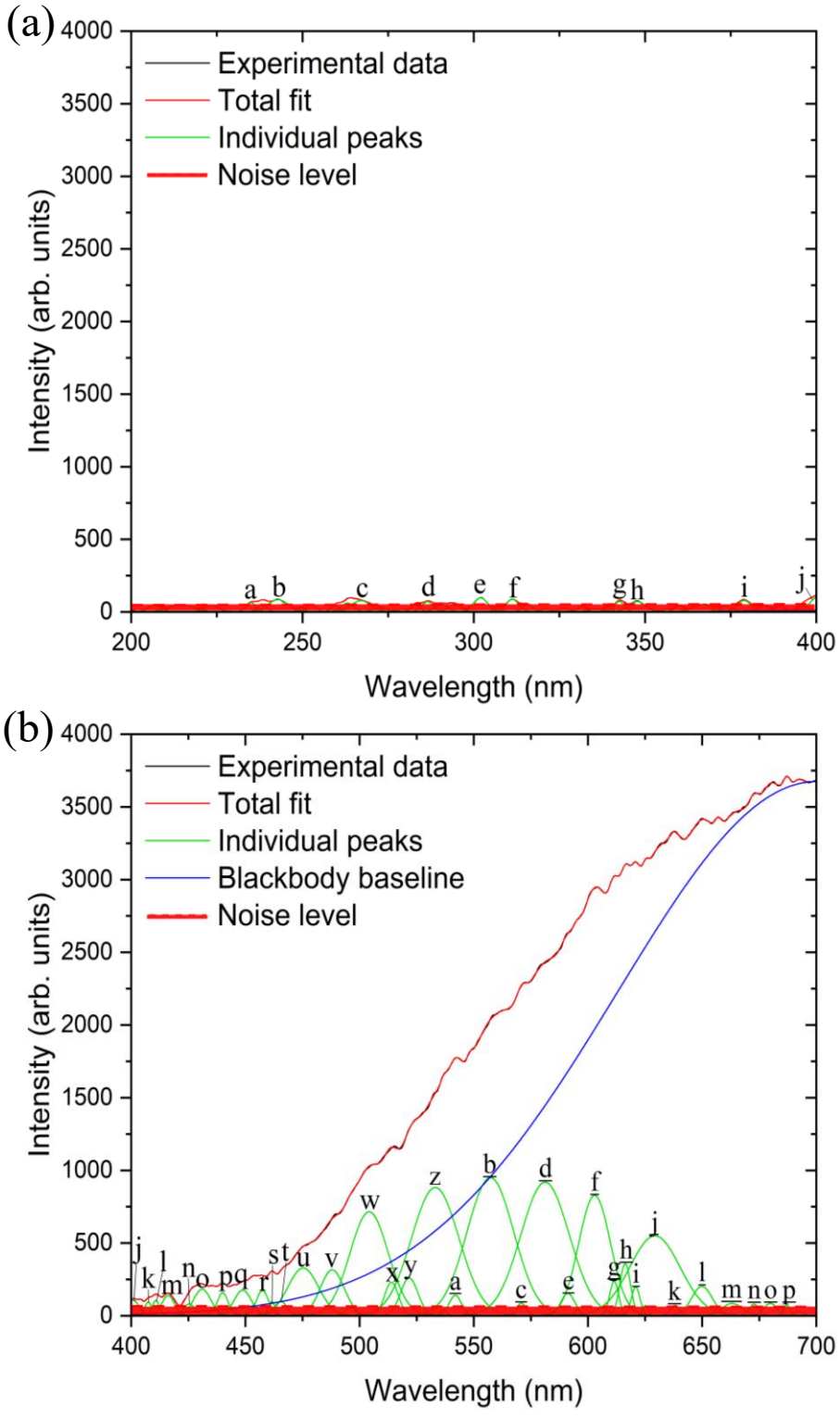

Figure S17. Deconvoluted UV-Vis emission spectrum of the levitated AIH particle in 40% O_2 and 60% Ar. (a) represents the wavelength region from 200 to 400 nm and (b) represents the wavelength region from 400 to 700 nm. See Table S3 for peak assignments.

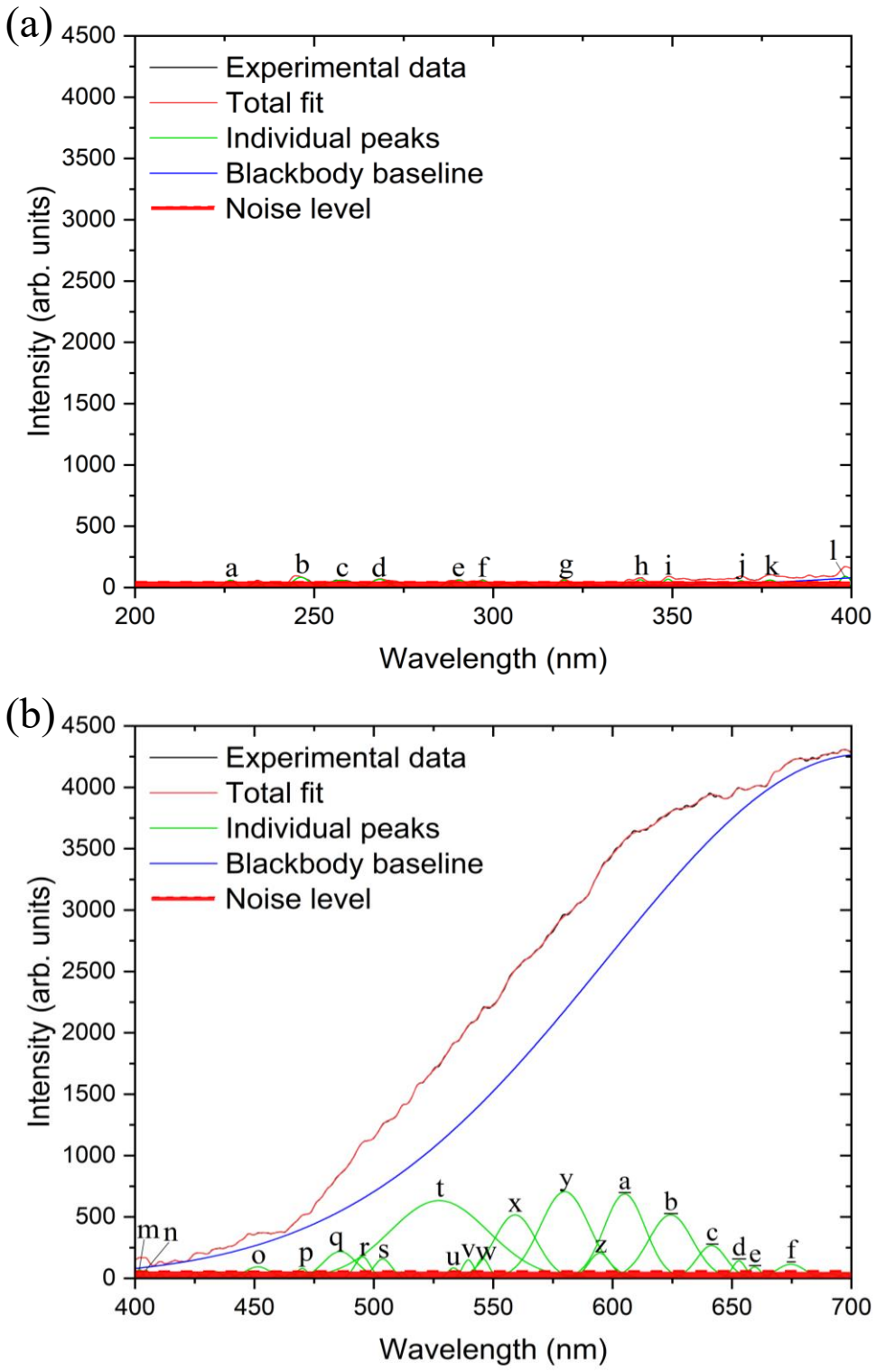

Figure S18. Deconvoluted UV-Vis emission spectrum of the levitated AIH particle in 50% O_2 and 50% Ar. (a) represents the wavelength region from 200 to 400 nm and (b) represents the wavelength region from 400 to 700 nm. See Table S4 for peak assignments.

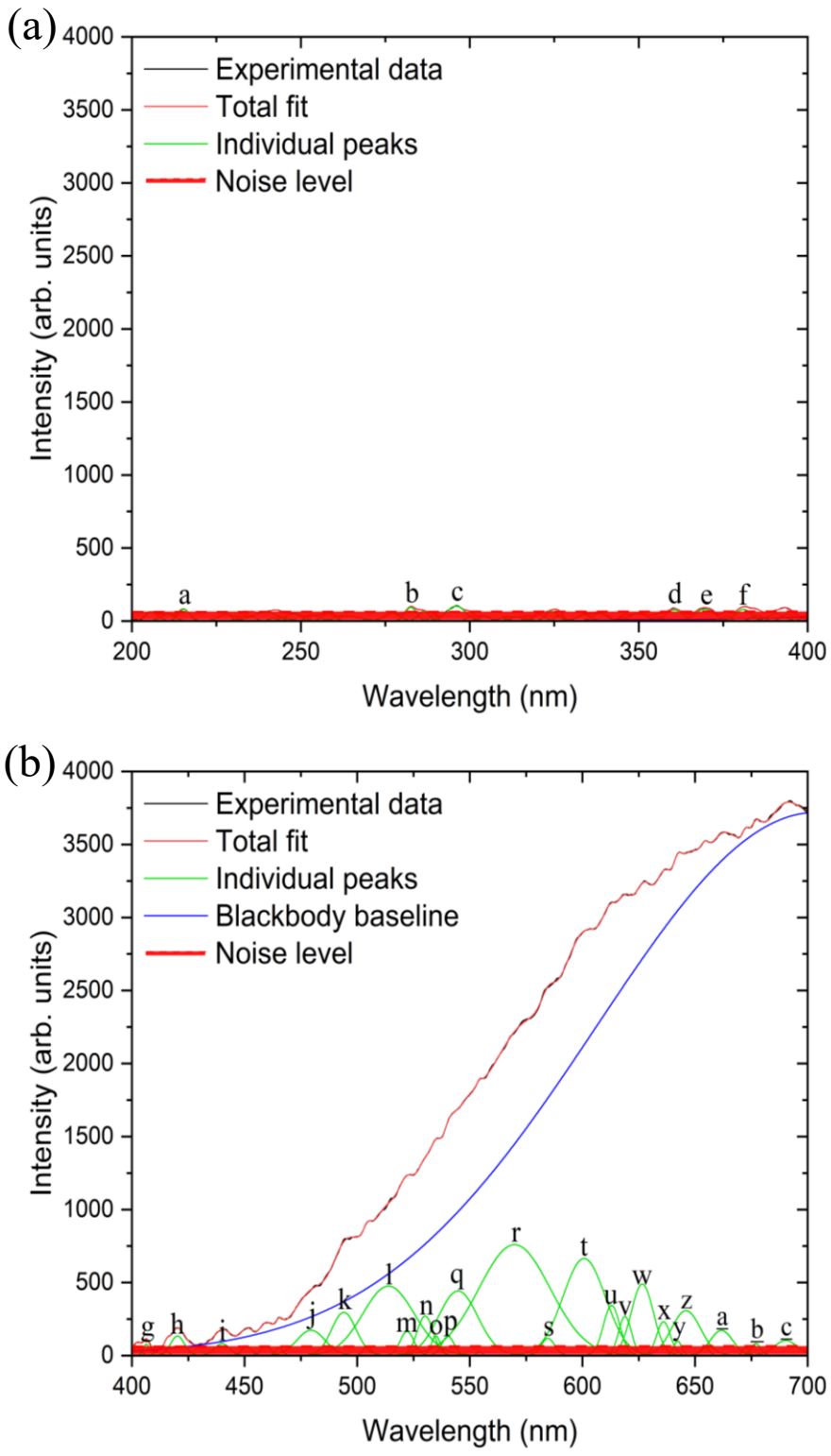

Figure S19. Deconvoluted UV-Vis emission spectrum of the levitated AIH particle in 60% O_2 and 40% Ar. (a) represents the wavelength region from 200 to 400 nm and (b) represents the wavelength region from 400 to 700 nm. See Table S5 for peak assignments.

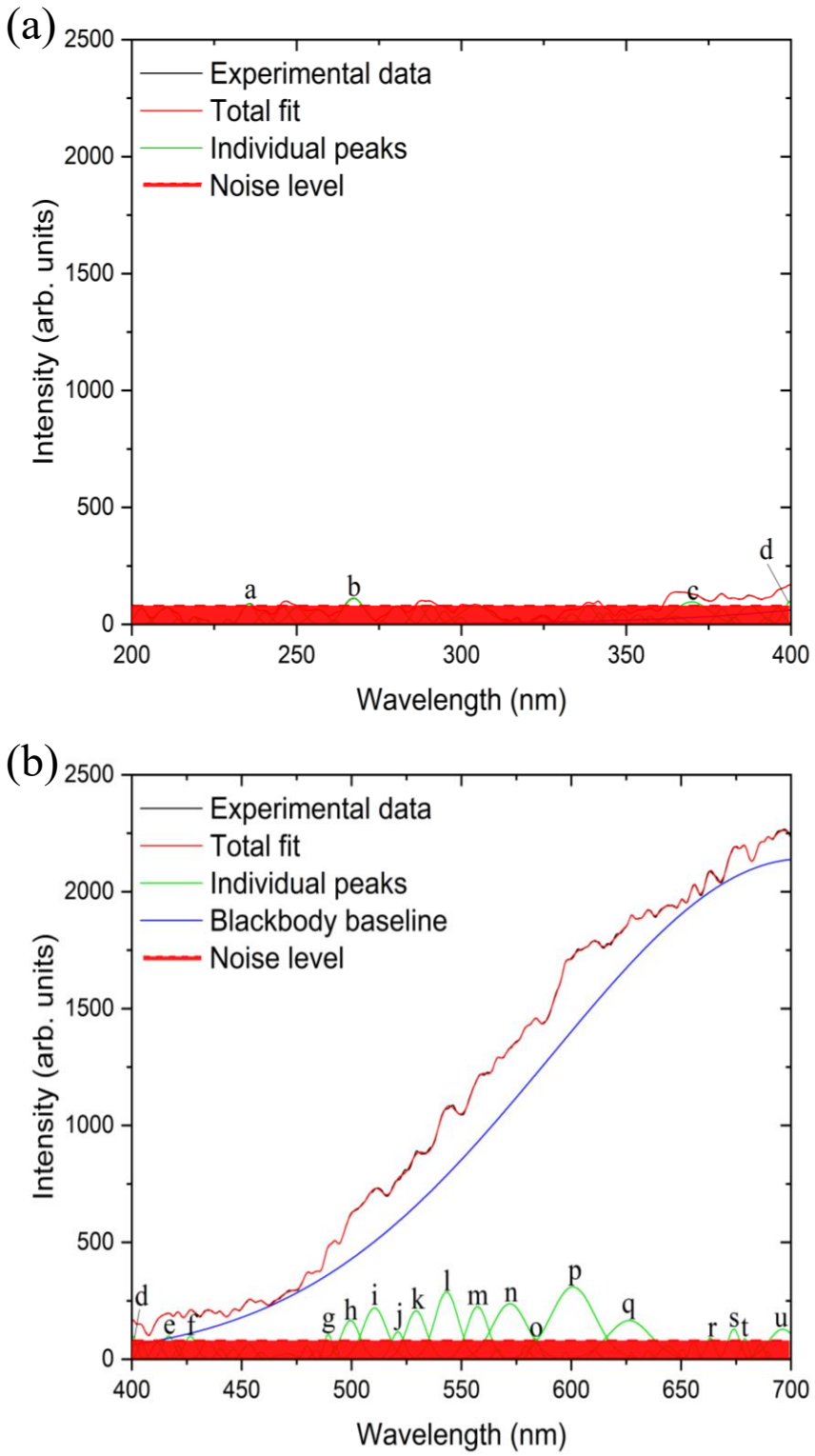

Figure S20. Deconvoluted UV-Vis emission spectrum of the levitated AIH particle in 70% O_2 and 30% Ar. (a) represents the wavelength region from 200 to 400 nm and (b) represents the wavelength region from 400 to 700 nm. See Table S6 for peak assignments.

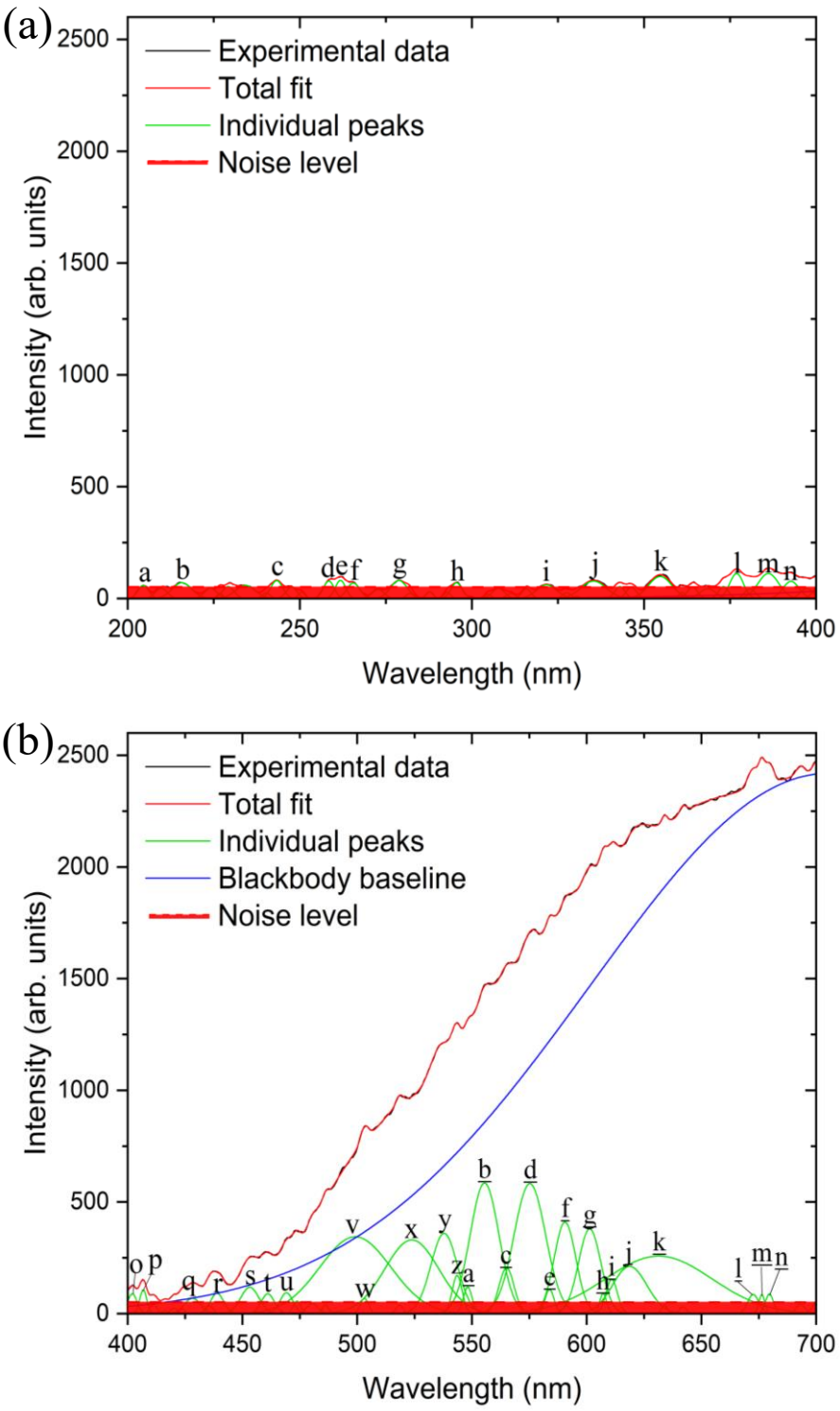

Figure S21. Deconvoluted UV-Vis emission spectrum of the levitated AIH particle in 80% O_2 and 20% Ar. (a) represents the wavelength region from 200 to 400 nm and (b) represents the wavelength region from 400 to 700 nm. See Table S7 for peak assignments.

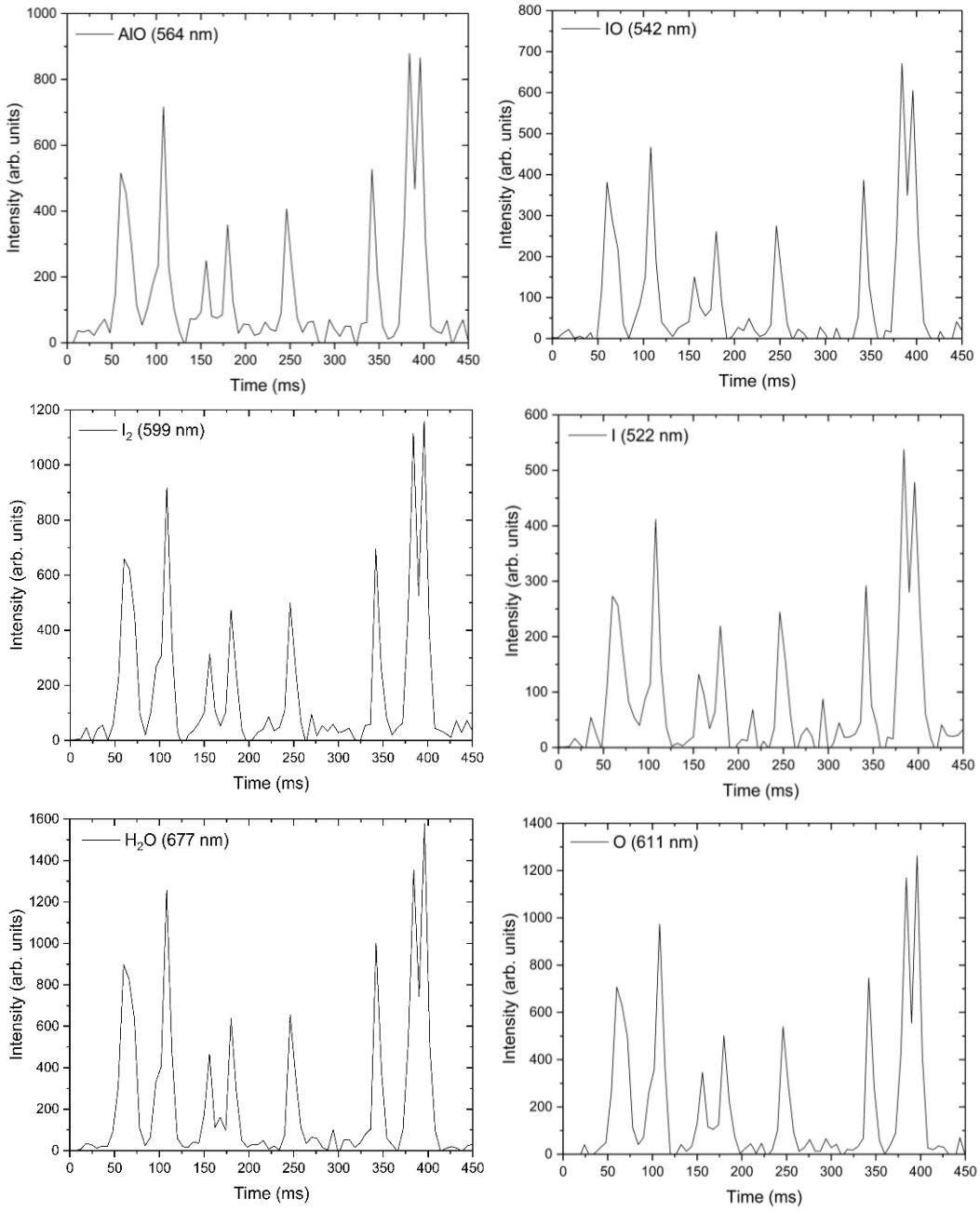

Figure S22. Emission profiles from the most intense peaks of each individual species in 10% O_2 and 90% Ar.

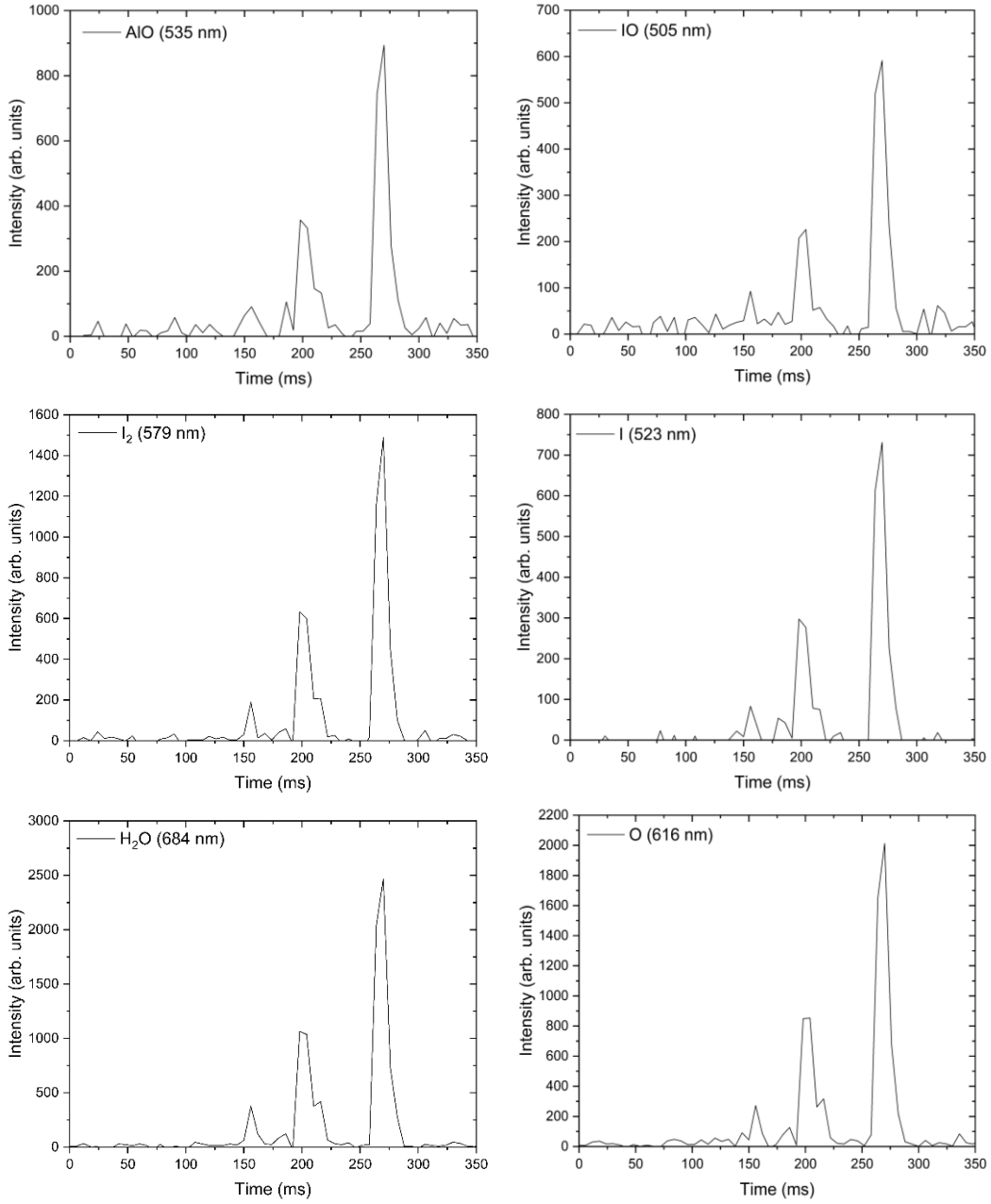

Figure S23. Emission profiles from the most intense peaks of each individual species in 20% O_2 and 80% Ar.

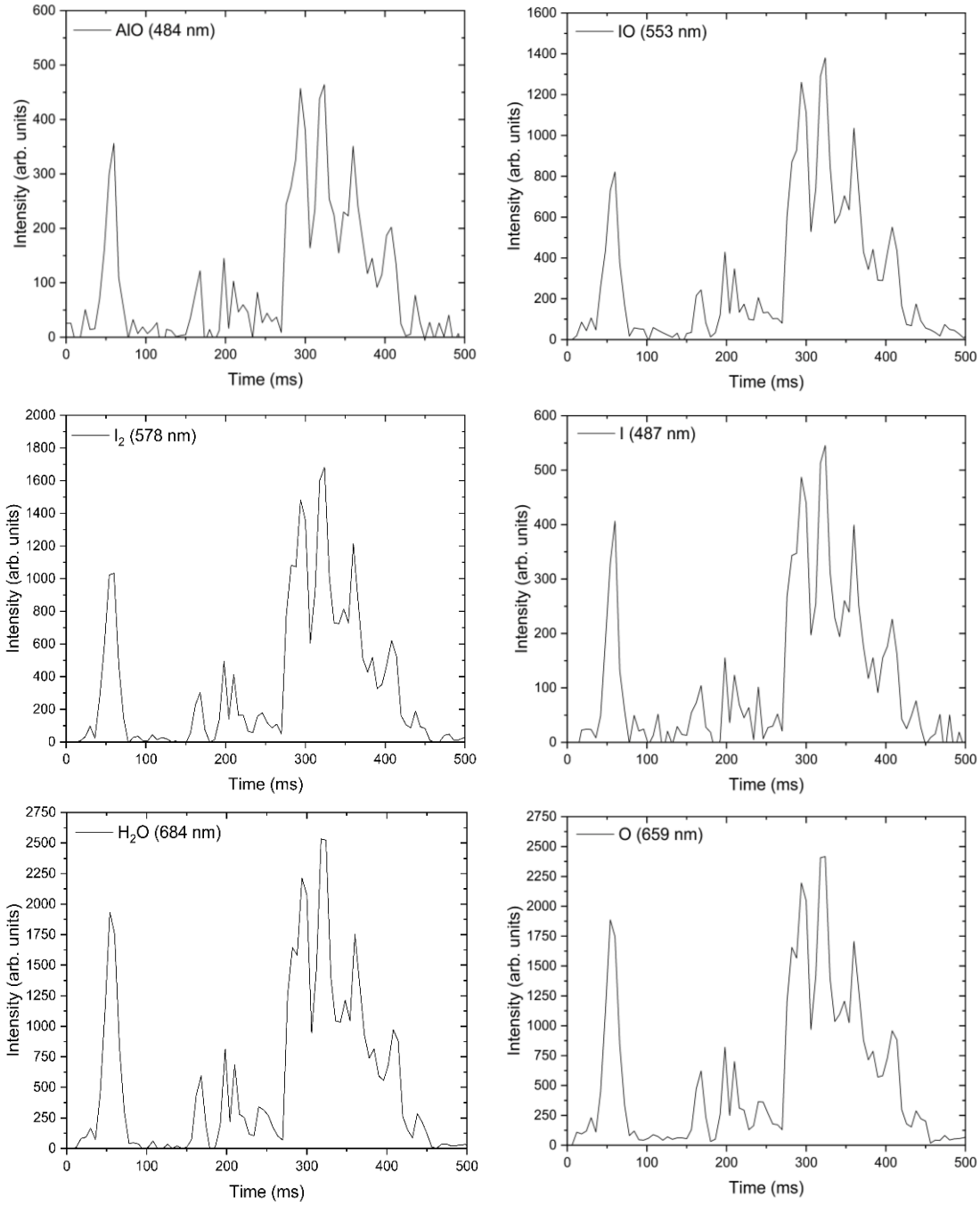

Figure S24. Emission profiles from the most intense peaks of each individual species in 30% O_2 and 70% Ar.

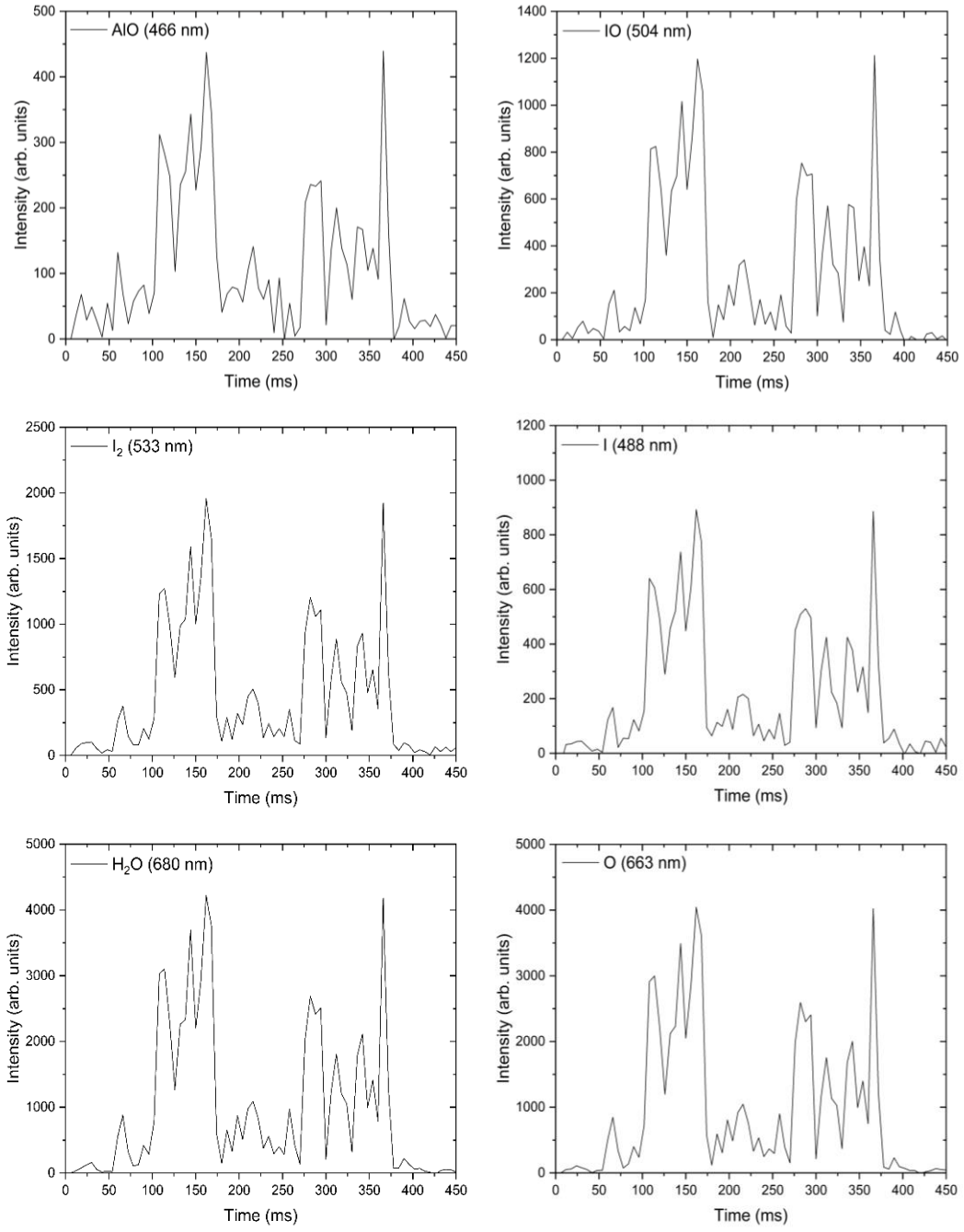

Figure S25. Emission profiles from the most intense peaks of each individual species in 40% O_2 and 60% Ar.

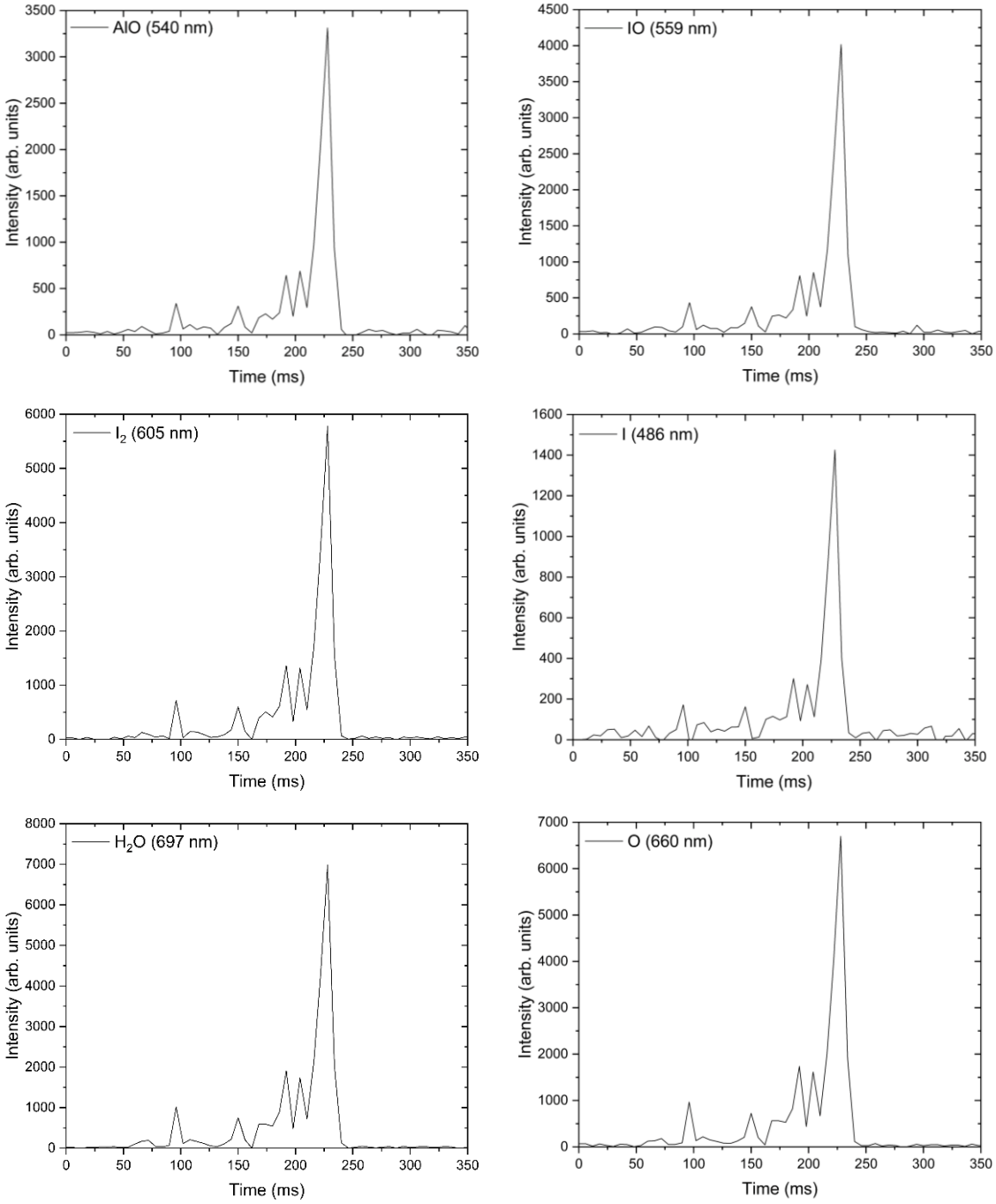

Figure S26. Emission profiles from the most intense peaks of each individual species in 50% O_2 and 50% Ar.

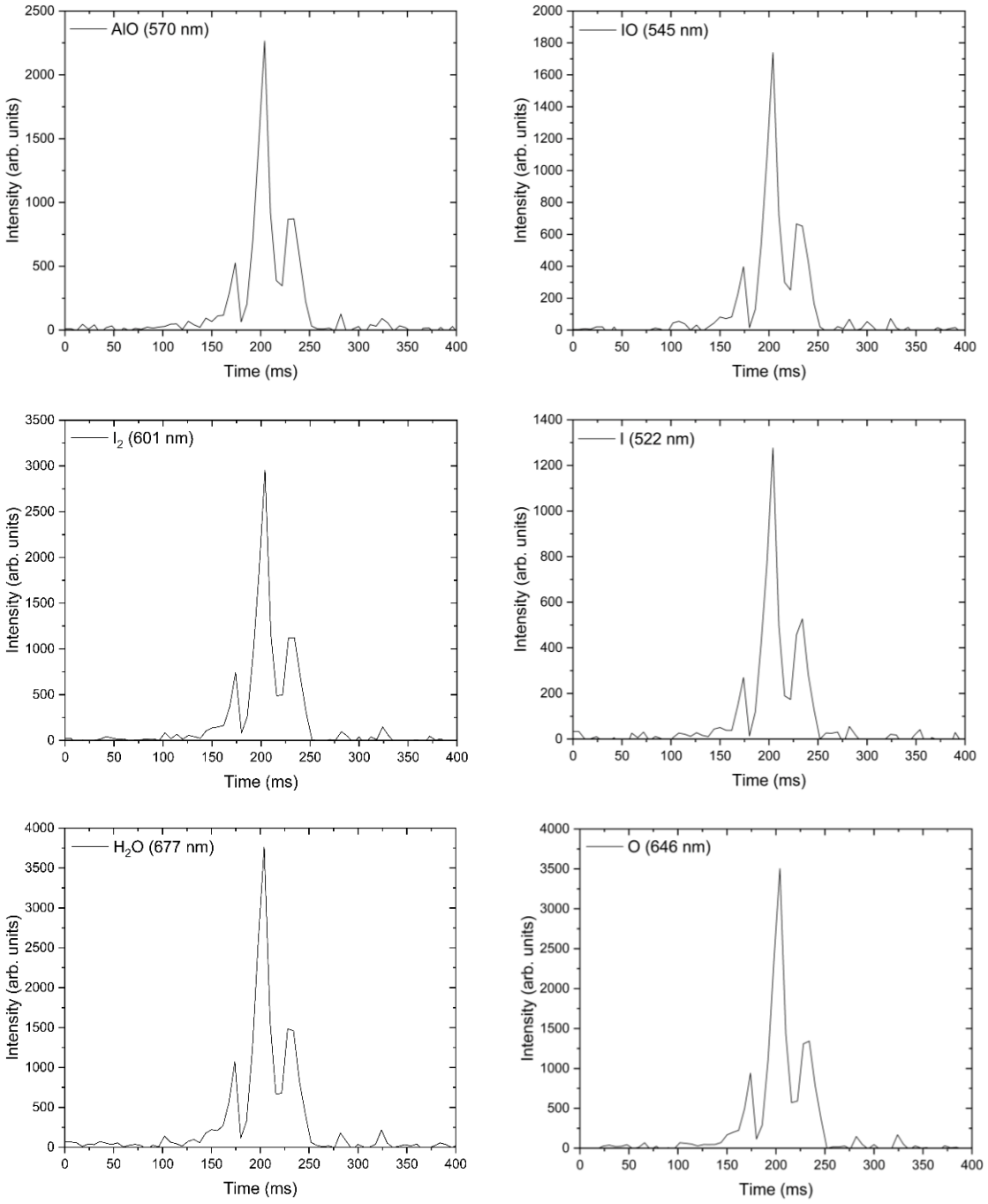

Figure S27. Emission profiles from the most intense peaks of each individual species in 60% O_2 and 40% Ar.

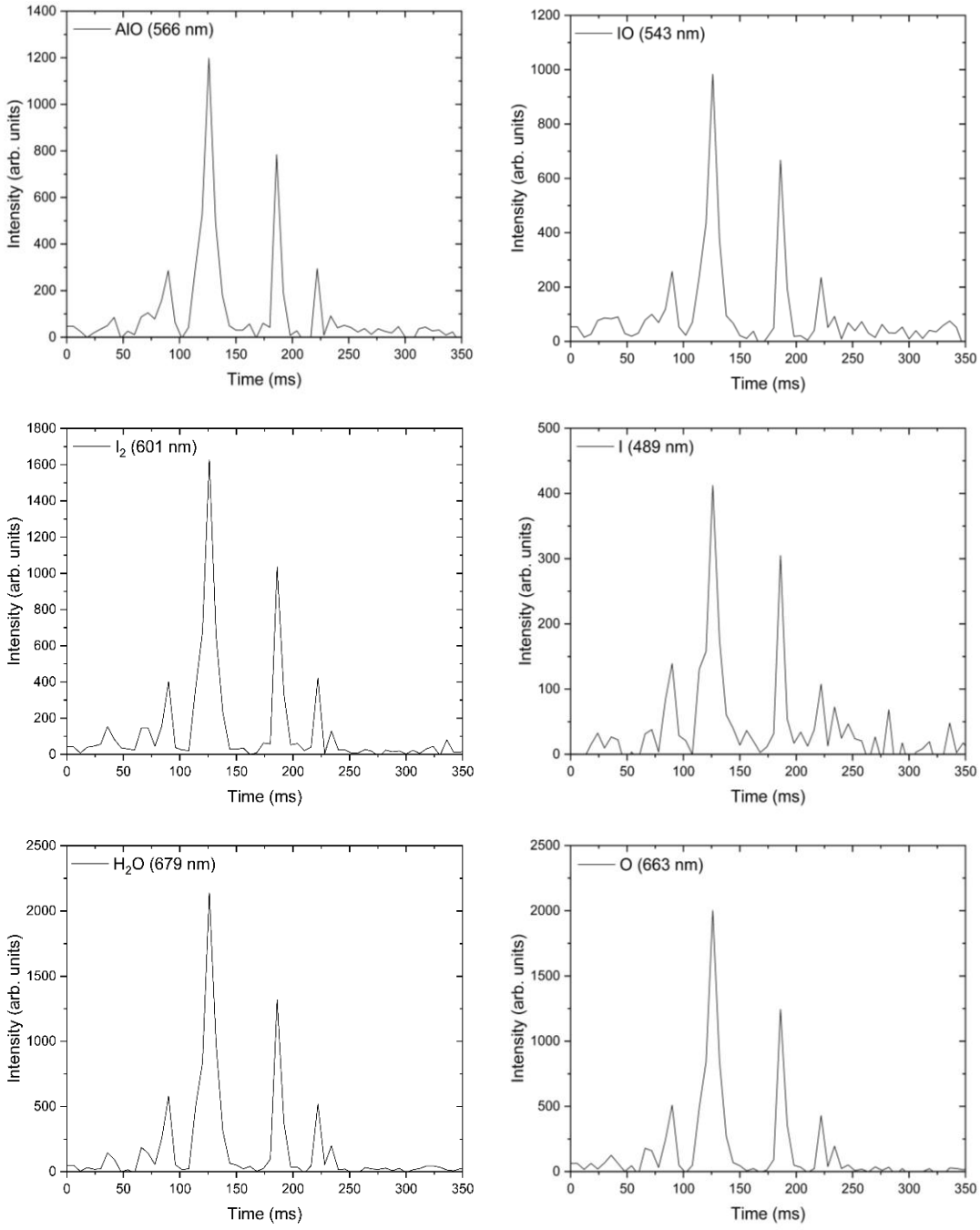

Figure S28. Emission profiles from the most intense peaks of each individual species in 70% O_2 and 30% Ar.

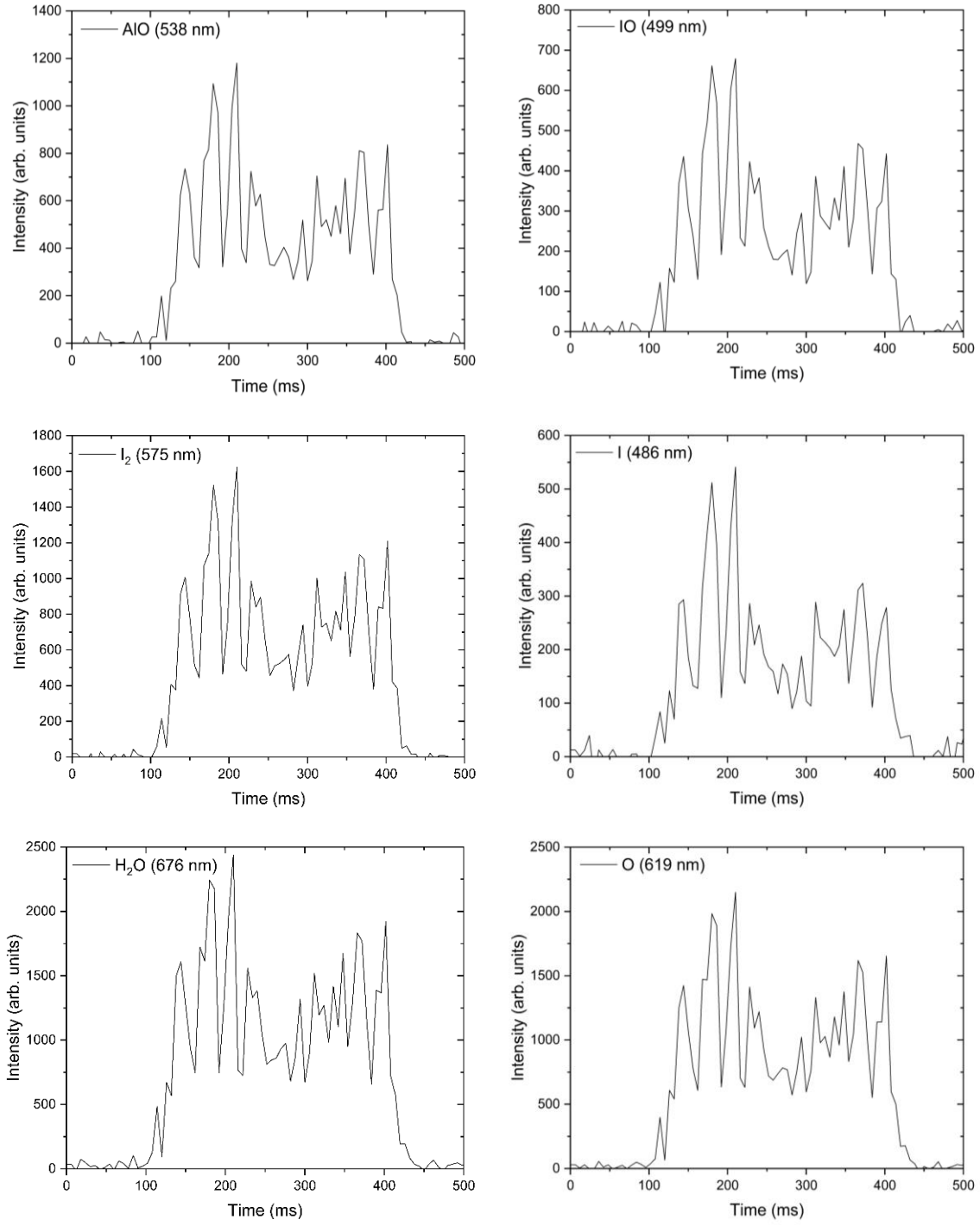

Figure S29. Emission profiles from the most intense peaks of each individual species in 80% O_2 and 20% Ar.

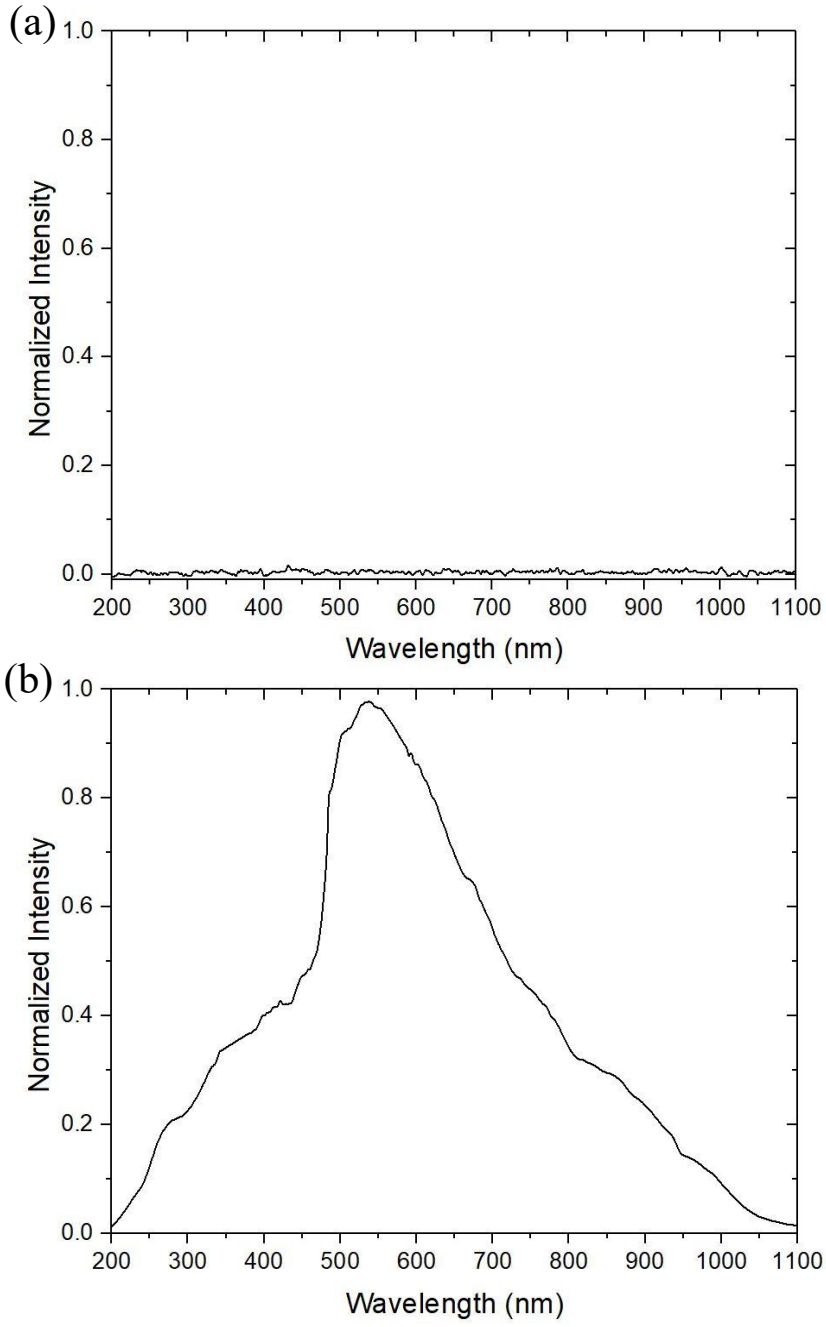

Figure S30. (a) Dark (background) spectrum and (b) the wavelength dependent detection sensitivity curve for the UV-Vis spectrometer and fiber optic probe combined.

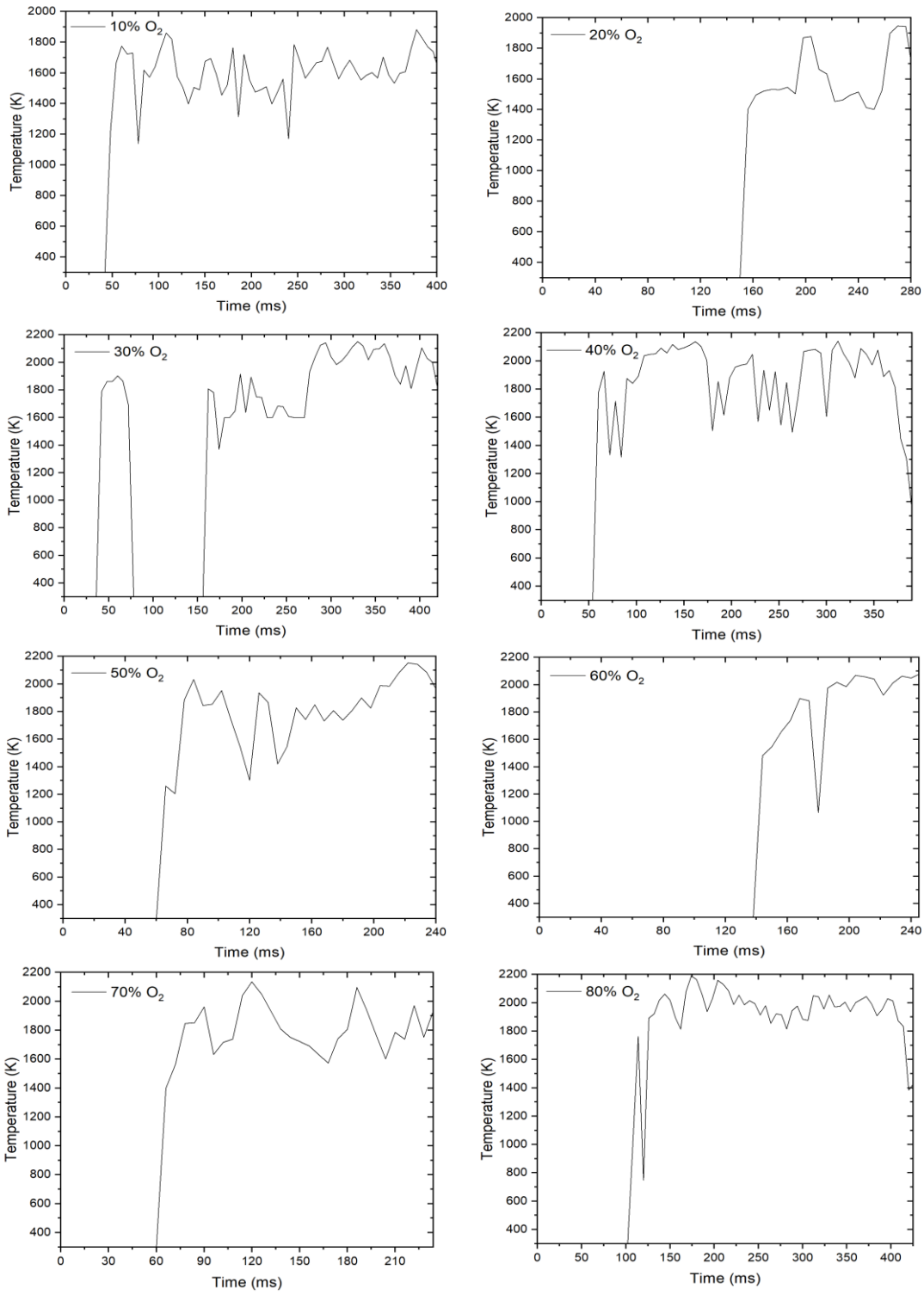

Figure S31. Temperature time profiles for the ignition of an AIH particle in 10%, 20%, 30%, 40%, 50%, 60%, 70%, and 80% O_2.

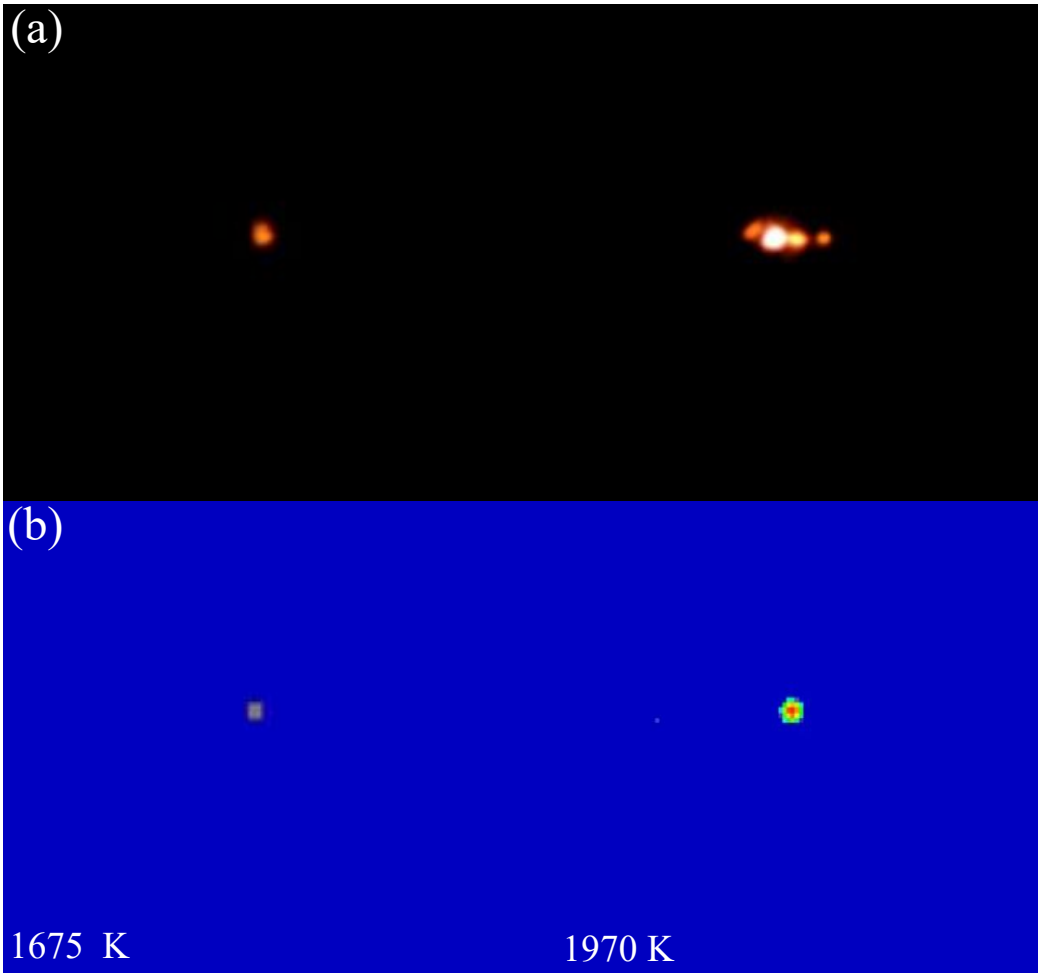

Figure S32. Optical and IR camera images taken during the levitation of AID in 20% O_2 and 80% Ar. (a) represents the optical images taken during ignition. The image on the left at the beginning of the ignition and the right is point of the ignition where it is most intense. (b) represents the respective IR camera images to the images shown in (a). The respective temperatures are shown at the bottom of (b).

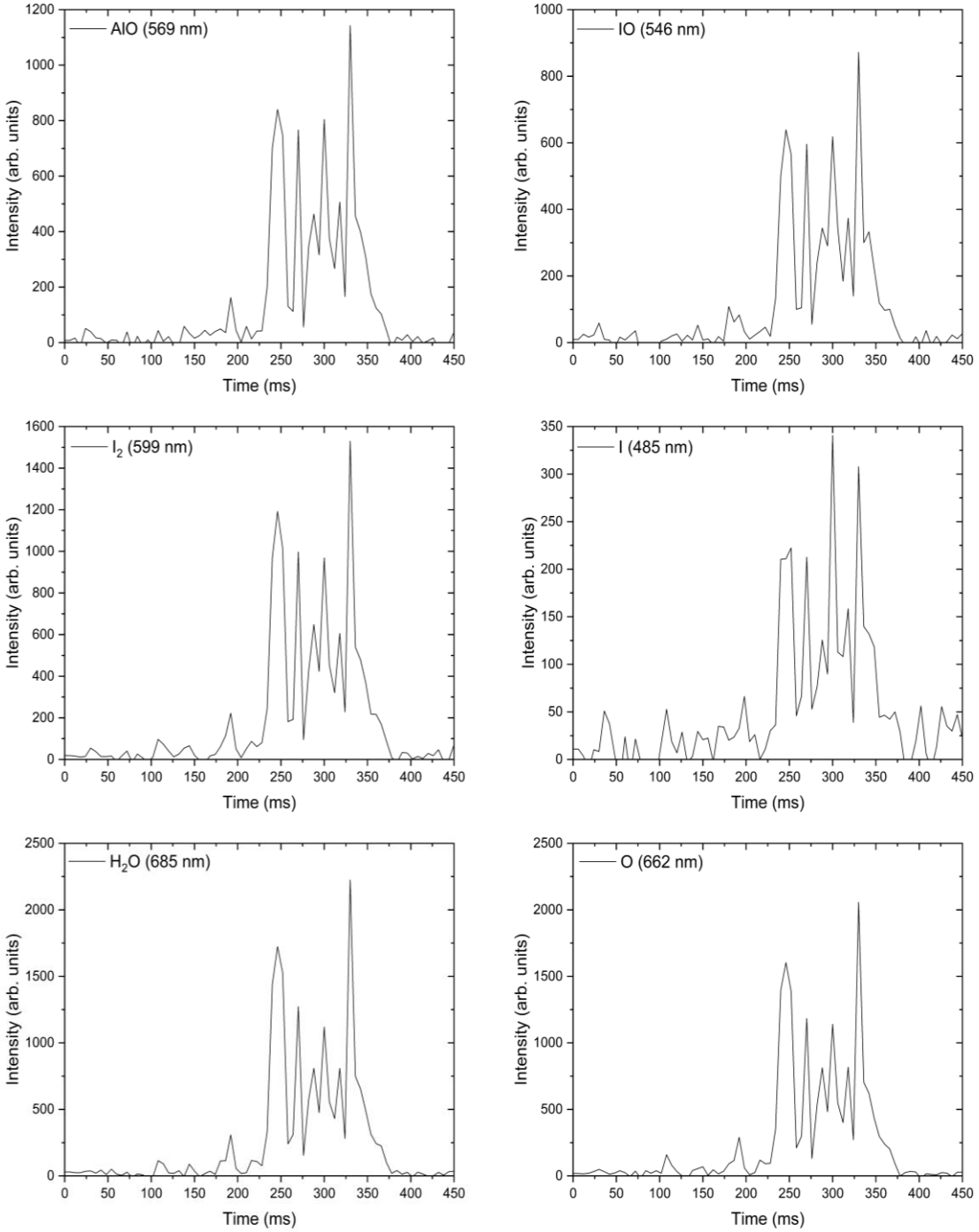

Figure S33. Emission profiles from the most intense peaks of each individual species in AID levitated in 20% O_2 and 80% Ar.

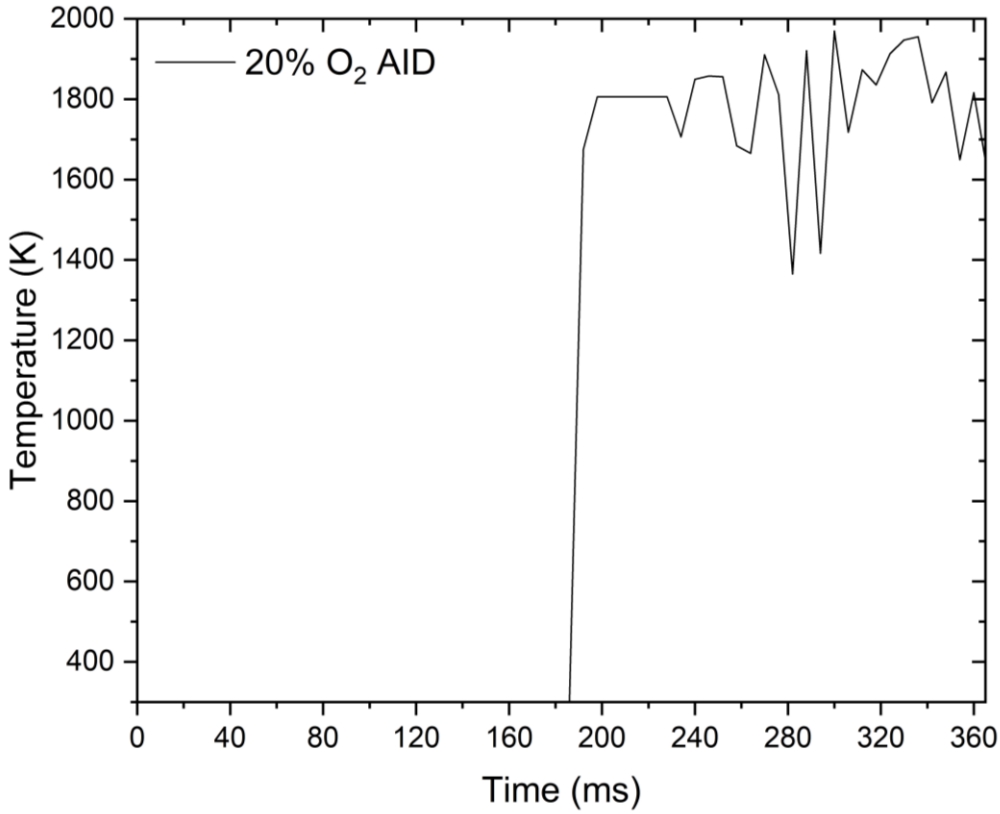

Figure S34. Temperature time profile for the ignition of an AID particle in 20% O_2.

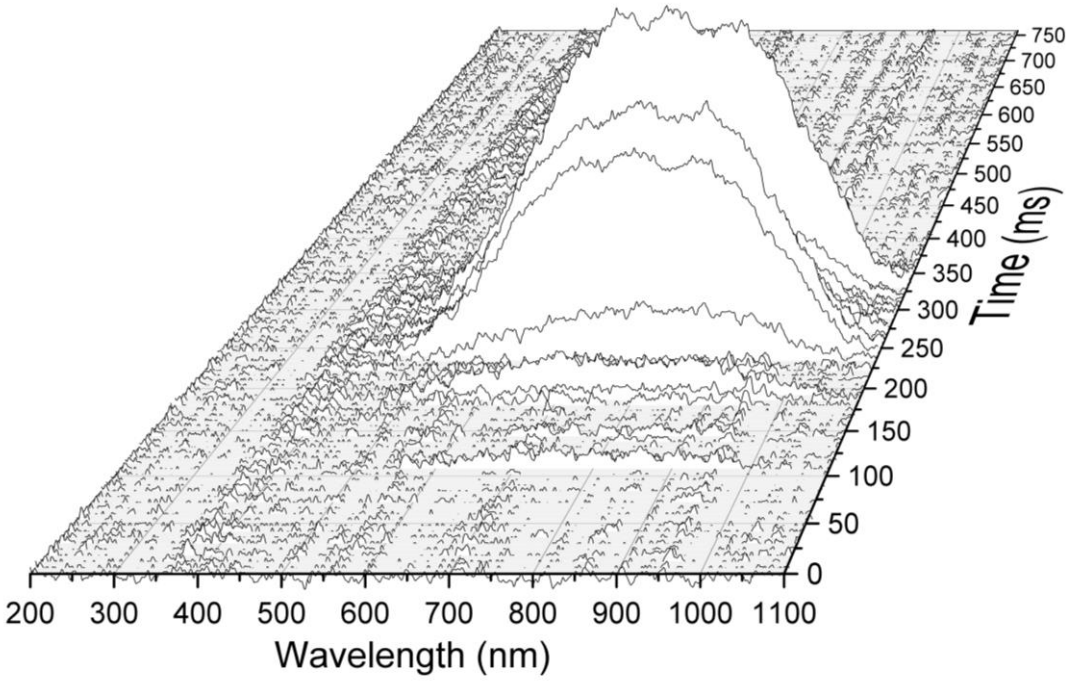

Figure S35. 3D plot of the AID emission spectra when levitated in 20% O_2 and 80% Ar.

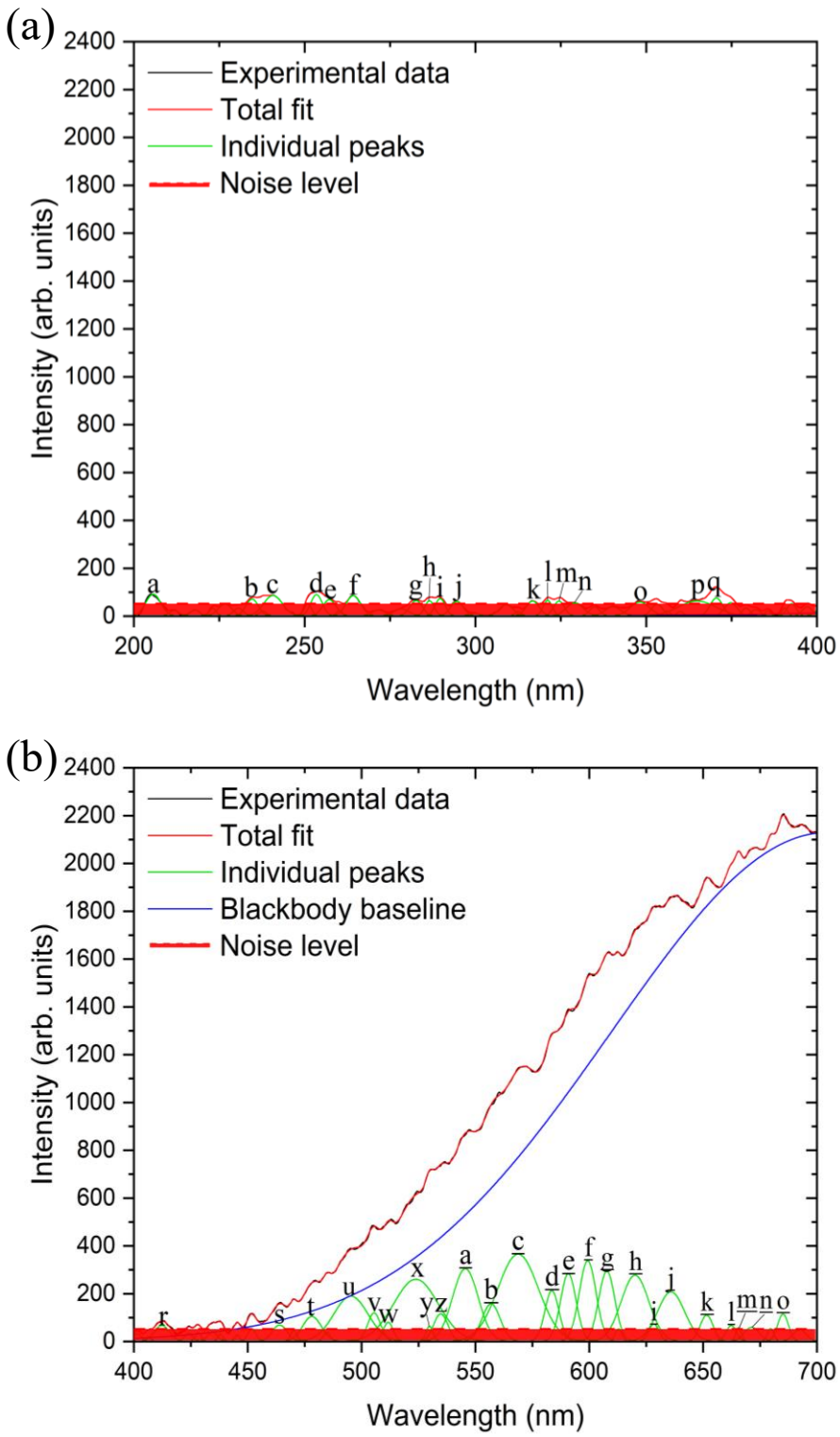

Figure S36. Deconvoluted UV-Vis emission spectrum of the levitated AID particle in 20% O_2 and 80% Ar. (a) represents the wavelength region from 200 to 400 nm and (b) represents the wavelength region from 400 to 700 nm. See Table S9 for peak assignments.

Table S1: Peak assignments for the deconvoluted emission spectrum of AlH particle levitated in 10% O_2 and 90% Ar

Peak/band	Peak wavelength/band center (nm)	Carrier	Reference wavelength (nm)[22,23,24]	Transition	Branch; spin-orbit components; vibrational quantum numbers: (ν', ν'') or (ν1',ν2',ν3') – (ν1'',ν2'',ν3'')
a	340.7	AlO Al Na	340 343 343	$C\ ^2\Pi - X\ ^2\Sigma^+$ $3p^2\ ^4P - 3p\ ^2P^o$ $3d\ ^2D - 3s\ ^2S$; $3d\ ^4F^o - 3p(^3P^o)\ ^4S$	(0,4) 3/2 – 1/2 3/2 – 1/2; 5/2 – 3/2
b	345.1	Al Na Na	344 343 348	$3p^2\ ^4P - 3p\ ^2P^o$ $3d\ ^2D - 3s\ ^2S$; $3d\ ^4F^o - 3p(^3P^o)\ ^4S$ $3d\ ^4D^o - 3p(^3P^o)\ ^4S$	5/2 – 3/2; 1/2 – 1/2 3/2 – 1/2; 5/2 – 3/2 5/2 – 3/2
c	352.6	Na	350 351	$3d\ ^4P^o - 3p(^3P^o)\ ^4S$	3/2 – 3/2; 1/2 – 3/2
d	366.1	Li K	367 364	$9d\ ^2D - 2p\ ^2P^o$ $4d\ ^2D - 4s\ ^2S$	3/2 – 1/2; 3/2 – 3/2; 5/2 – 3/2 3/2 – 1/2; 5/2 – 1/2
e	369.9	Li	371	$8d\ ^2D - 2p\ ^2P^o$	3/2 – 1/2; 5/2 – 3/2; 3/2 – 3/2
f	395.0	Al Al O	394 396 394	$4s\ ^2S - 3p\ ^2P^o$ $4s\ ^2S - 3p\ ^2P^o$ $4p\ ^5P - 3s\ ^5S^o$	1/2 – 1/2 1/2 – 3/2 3–2; 2–2; 1–2
g	441.5	IO	440	$A\ ^2\Pi_{3/2} - X\ ^2\Pi_{3/2}$	(2,1)
h	476.4	K	474	$13s\ ^2S - 4p\ ^2P^o$; $11d\ ^2D - 4p\ ^2P^o$	1/2 – 1/2; 3/2 – 1/2
i	481.0	I	476	$7p\ ^2[1]^o - 6s\ ^2[2]$	3/2 – 5/2
j	484.5	AlO	485	$B\ ^2\Sigma^+ - X\ ^2\Sigma^+$	(0,0)
k	496.0	K	496	$8d\ ^2D - 4p\ ^2P^o$	5/2 – 3/2
l	508.3	I_2	509	$B\ ^3\Pi_{0+u} - X\ ^1\Sigma_g^+$	(46,0)
m	512.7	AlO I	510 511	$B\ ^2\Sigma^+ - X\ ^2\Sigma^+$	(0,1) 3/2 – 3/2

				$7p\ ^2[1]^o - 6s\ ^2[2]$	
n	517.4	Na	516	$4s\ ^4P^o - 3p(^3P^o)\ ^4D$	5/2 – 5/2
o	521.8	I	523	$7p\ ^2[3]^o - 6s\ ^2[2]$	5/2 – 3/2
p	528.3	Na	525	$4s\ ^4P^o - 3p(^3P^o)\ ^4D$	5/2 – 3/2
q	541.7	I I_2	542 545	$6p\ ^2[1]^o - 6s\ ^2[2]$ $B\ ^3\Pi_{0+u} - X\ ^1\Sigma_g^+$	3/2 – 5/2 (25,0)
r	564.3	AlO	565	$B\ ^2\Sigma^+ - X\ ^2\Sigma^+$	(2,5)
s	583.0	I_2	585	$B\ ^3\Pi_{0+u} - X\ ^1\Sigma_g^+$	(16,2)
t	592.1	I_2 Na	592 589	$B\ ^3\Pi_{0+u} - X\ ^1\Sigma_g^+$ $3p\ ^2P^o - 3s\ ^2S$	(14,2) 1/2 – 1/2
u	598.6	I_2	600	$B\ ^3\Pi_{0+u} - X\ ^1\Sigma_g^+$	(12,2)
v	611.1	I_2 Li O	611 610 615	$B\ ^3\Pi_{0+u} - X\ ^1\Sigma_g^+$ $3d\ ^2D - 2p\ ^2P^o$ $4d\ ^5D^o - 3p\ ^5P$	(11,3) 3/2 – 1/2; 5/2 – 3/2; 3/2 – 3/2 1–1; 3–2; 4–3
w	638.2	I_2	636	$B\ ^3\Pi_{0+u} - X\ ^1\Sigma_g^+$	(7,4)

Table S2: Peak assignments for the deconvoluted emission spectrum of AlH particle levitated in 30% O_2 and 70% Ar

Peak/band	Peak wavelength/band center (nm)	Carrier	Reference wavelength (nm)[22,23,24]	Transition	Branch; spin-orbit components; vibrational quantum numbers: (ν', ν'') or (ν1',ν2',ν3') – (ν1'',ν2'',ν3'')
a	217.7	Al	215	8d ^{2}D – 3p ^{2}P^o	5/2 – 3/2; 3/2 – 3/2
b	245.7	AlO	245	D $^2\Sigma^+$ – X $^2\Sigma^+$	(1,0)
c	299.2	AlO O	296 297	C $^2\Pi$ – X $^2\Sigma^+$ 2p^4 ^{1}S – 2p^4 ^{3}P	(1,0) 0 – 1
d	308.8	OH Al	310 309	A $^2\Sigma^+$– X $^2\Pi$ 3d ^{2}D – 3p ^{2}P^o	(0-0), (1-1) 5/2 – 3/2; 3/2 – 3/2
e	333.9	AlO	332	C $^2\Pi$ – X $^2\Sigma^+$	(2,5)
f	398.2	Al Al O	396 394 394	4s ^{2}S – 3p ^{2}P^o 4s ^{2}S – 3p ^{2}P^o 4p ^{5}P – 3s ^{5}S^o	1/2 – 3/2 1/2 – 1/2 3–2; 2–2; 1–2
g	428.2	Na Al	425 425	3d ^{4}D^o – 3p(^{3}P^o) ^{4}P 3d ^{2}D^o – 5d ^{2}D	5/2 – 3/2 5/2 – 5/2
h	437.0	IO	440	A $^2\Pi_{3/2}$ – X $^2\Pi_{3/2}$	(2,1)
i	454.9	AlO	451	B $^2\Sigma^+$– X $^2\Sigma^+$	(3,1)
j	463.0	Li	460	4d ^{2}D – 2p ^{2}P^o	3/2 – 1/2; 5/2 – 3/2; 3/2 – 3/2
k	470.5	AlO	467	B $^2\Sigma^+$– X $^2\Sigma^+$	(1,0)
l	479.9	I	476	7p ^{2}[1]^o – 6s ^{2}[2]	3/2 – 5/2
m	484.1	AlO	485	B $^2\Sigma^+$– X $^2\Sigma^+$	(0,0)
n	487.0	I	486	7p ^{2}[3]^o – 6s ^{2}[2]	7/2 – 5/2
o	491.9	I	491	7p ^{2}[2]^o – 6s ^{2}[2]	5/2 – 5/2
p	500.8	K	496	8d ^{2}D – 4p ^{2}P^o	5/2 – 3/2
q	509.9	I_2	509	B $^3\Pi_{0+u}$ – X $^1\Sigma_g^+$	(46,0)
r	529.5	Na	525	4s ^{4}P^o – 3p(^{3}P^o) ^{4}D	5/2 – 3/2
s	543.4	I I_2	542 545	6p ^{2}[1]^o – 6s ^{2}[2] B $^3\Pi_{0+u}$ – X $^1\Sigma_g^+$	3/2 – 5/2 (25,0)
t	552.7	IO	550	A $^2\Pi_{3/2}$ – X $^2\Pi_{3/2}$	(2,5)
u	577.6	I_2	578	B $^3\Pi_{0+u}$ – X $^1\Sigma_g^+$	(16,1)

v	585.4	I_2 Na	585 588	B $^3\Pi_{0+u}$ – X $^1\Sigma_g^+$ 3p $^2P^o$ – 3s ^2S	(16,2) 3/2 – 1/2
w	590.7	I_2 Na	592 589	B $^3\Pi_{0+u}$ – X $^1\Sigma_g^+$ 3p $^2P^o$ – 3s ^2S	(14,2) 1/2 – 1/2
x	596.5	I_2 AlO	596 595	B $^3\Pi_{0+u}$ – X $^1\Sigma_g^+$ B $^2\Sigma^+$ – X $^2\Sigma^+$	(13,2) (2,6)
y	610.7	I_2 Li	611 610	B $^3\Pi_{0+u}$ – X $^1\Sigma_g^+$ 3d ^2D – 2p $^2P^o$	(11,3) 3/2 – 1/2; 5/2 – 3/2; 3/2 – 3/2
z	624.4	I_2	623	B $^3\Pi_{0+u}$ – X $^1\Sigma_g^+$	(10,4)
a	632.2	I_2	632	B $^3\Pi_{0+u}$ – X $^1\Sigma_g^+$	(8,4)
b	638.0	I_2	636	B $^3\Pi_{0+u}$ – X $^1\Sigma_g^+$	(7,4)
c	645.2	I_2 O	641 645	B $^3\Pi_{0+u}$ – X $^1\Sigma_g^+$ 5s $^5S^o$ – 3p ^5P	(8,5) 2–1; 2–2; 2–3
d	653.2	I_2	654	B $^3\Pi_{0+u}$ – X $^1\Sigma_g^+$	(7,6)
e	658.8	O	660	5s $^1D^o$ – 3p ^1F	2–3
f	667.9	I_2	664	B $^3\Pi_{0+u}$ – X $^1\Sigma_g^+$	(5,6)
g	675.2	H_2O Li	632-683 670	ro-vib. mode 2p $^2P^o$ – 2s ^2S	(1,1,3) – (1,5,1) 3/2 – 1/2; 1/2 – 1/2
h	683.5	H_2O	632-683	ro-vib. mode	(1,1,3) – (1,5,1)
i	692.2	H_2O K	690-710 693	ro-vib. mode 4d ^2D – 4p $^2P^o$; 6s ^2S – 4p $^2P^o$	(1,0,3) – (0,0,0) 3/2 – 1/2; 1/2 – 3/2

Table S3: Peak assignments for the deconvoluted emission spectrum of AlH particle levitated in 40% O_2 and 60% Ar

Peak/band	Peak wavelength/band center (nm)	Carrier	Reference wavelength (nm)[22,23,24]	Transition	Branch; spin-orbit components; vibrational quantum numbers: (ν', ν'') or (ν1',ν2',ν3') – (ν1'',ν2'',ν3'')
a	235.0	AlO	235	$D\ ^2\Sigma^+ - X\ ^2\Sigma^+$	(3,0)
b	242.9	Li	242	$7p\ ^2P^o - 2s\ ^2S$	3/2 – 1/2; 1/2 – 1/2
c	267.0	AlO	269	$D\ ^2\Sigma^+ - X\ ^2\Sigma^+$	(1,4)
d	286.5	OH Na	287 – 289 285	$A\ ^2\Sigma^+ - X\ ^2\Pi$ $5p\ ^2P^o - 3s\ ^2S$	R_1, R_2, Q_1, Q_2; (2, 1) 3/2 – 1/2; 1/2 – 1/2
e	302.0	AlO	303	$C\ ^2\Pi - X\ ^2\Sigma^+$	(0,0)
f	311.3	OH	310	$A\ ^2\Sigma^+ - X\ ^2\Pi$	(0-0), (1-1)
g	342.5	Al Na Al	343 343 344	$3p^2\ ^4P - 3p\ ^2P^o$ $3d\ ^2D - 3s\ ^2S$; $3d\ ^4F^o - 3p(^3P^o)\ ^4S$ $3p^2\ ^4P - 3p\ ^2P^o$	3/2 – 1/2 3/2 – 1/2; 5/2 – 3/2 5/2 – 3/2; 1/2 – 1/2
h	347.7	Na	348	$3d\ ^4D^o - 3p(^3P^o)\ ^4S$	5/2 – 3/2
i	378.9	Li	379	$7d\ ^2D - 2p\ ^2P^o$	3/2 – 1/2; 5/2 – 3/2; 3/2 – 3/2
j	400.8	Al	396	$4s\ ^2S - 3p\ ^2P^o$	1/2 – 3/2
k	407.5	K	404	$5p\ ^2P^o - 4s\ ^2S$	3/2 – 1/2; 1/2 – 1/2
l	410.8	I	410	$6p\ ^2[3]^o - 6s\ ^2[2]$	7/2 – 5/2
m	416.2	Na	418	$3d\ ^4D^o - 3p(^3P^o)\ ^4P$	5/2 – 5/2
n	425.4	Na Al	425 425	$3d\ ^4D^o - 3p(^3P^o)\ ^4P$ $3d\ ^2D^o - 5d\ ^2D$	5/2 – 3/2 5/2 – 5/2
o	431.1	Na	432	$9d\ ^2D - 3p\ ^2P^o$	3/2 – 1/2; 3/2 – 3/2; 5/2 – 3/2
p	440.0	IO	440	$A\ ^2\Pi_{3/2} - X\ ^2\Pi_{3/2}$	(2,1)
q	448.8	AlO	451	$B\ ^2\Sigma^+ - X\ ^2\Sigma^+$	(3,1)
r	457.5	Li	460	$4d\ ^2D - 2p\ ^2P^o$	3/2 – 1/2; 5/2 – 3/2; 3/2 – 3/2
s	461.6	K	464	$3d\ ^2D - 4s\ ^2S$	5/2 – 1/2
t	465.5	AlO	467	$B\ ^2\Sigma^+ - X\ ^2\Sigma^+$	(1,0)

u	475.3	K	474	13s ^{2}S – 4p ^{2}P^o; 11d ^{2}D – 4p ^{2}P^o	1/2 – 1/2; 3/2 – 1/2
v	488.0	AlO I	485 486	B $^2\Sigma^+$– X $^2\Sigma^+$ 7p ^{2}[3]^o – 6s ^{2}[2]	(0,0) 7/2 – 5/2
w	504.2	Na	507	4s ^{4}P^o – 3p(^{3}P^o) ^{4}D	7/2 – 5/2
x	514.0	Na	516	4s ^{4}P^o – 3p(^{3}P^o) ^{4}D	5/2 – 5/2
y	521.7	I	523	7p ^{2}[3]^o – 6s ^{2}[2]	5/2 – 3/2
z	533.1	I_2	532	B $^3\Pi_{0+u}$ – X $^1\Sigma_g^+$	(32,0)
a	541.9	I I_2	542 545	6p ^{2}[1]^o – 6s ^{2}[2] B $^3\Pi_{0+u}$ – X $^1\Sigma_g^+$	3/2 – 5/2 (25,0)
b	557.3	Na Al	556 555	4s ^{4}P^o – 3p(^{3}P^o) ^{4}P 6p ^{2}P^o – 4s ^{2}S	3/2 – 3/2 3/2 – 1/2; 1/2 – 1/2
c	570.9	I_2	574	B $^3\Pi_{0+u}$ – X $^1\Sigma_g^+$	(17,1)
d	581.2	I_2	585	B $^3\Pi_{0+u}$ – X $^1\Sigma_g^+$	(16,2)
e	591.2	I_2 Na	592 589	B $^3\Pi_{0+u}$ – X $^1\Sigma_g^+$ 3p ^{2}P^o – 3s ^{2}S	(14,2) 1/2 – 1/2
f	602.9	I_2	600	B $^3\Pi_{0+u}$ – X $^1\Sigma_g^+$	(12,2)
g	611.5	I_2 Li	611 610	B $^3\Pi_{0+u}$ – X $^1\Sigma_g^+$ 3d ^{2}D – 2p ^{2}P^o	(11,3) 3/2 – 1/2; 5/2 – 3/2; 3/2 – 3/2
h	616.3	I_2 O	615 615	B $^3\Pi_{0+u}$ – X $^1\Sigma_g^+$ 4d ^{5}D^o – 3p ^{5}P	(10,3) 1–1; 3–2; 4–3
i	620.9	I_2	619	B $^3\Pi_{0+u}$ – X $^1\Sigma_g^+$	(9,3)
j	629.3	I_2	628	B $^3\Pi_{0+u}$ – X $^1\Sigma_g^+$	(9,4)
k	638.1	I_2	636	B $^3\Pi_{0+u}$ – X $^1\Sigma_g^+$	(7,4)
l	649.9	I_2	649	B $^3\Pi_{0+u}$ – X $^1\Sigma_g^+$	(8,6)
m	663.1	O I_2	660 664	5s ^{1}D^o – 3p ^{1}F B $^3\Pi_{0+u}$ – X $^1\Sigma_g^+$	2–3 (5,6)
n	672.7	H_2O Li	632-683 670	ro-vib. mode 2p ^{2}P^o – 2s ^{2}S	(1,1,3) – (1,5,1) 3/2 – 1/2; 1/2 – 1/2
o	679.9	H_2O	632-683	ro-vib. mode	(1,1,3) – (1,5,1)
p	687.0	H_2O	690-710	ro-vib. mode	(1,0,3) – (0,0,0)

Table S4: Peak assignments for the deconvoluted emission spectrum of AlH particle levitated in 50% O_2 and 50% Ar

Peak/band	Peak wavelength/band center (nm)	Carrier	Reference wavelength (nm)[22,23,24]	Transition	Branch; spin-orbit components; vibrational quantum numbers: (ν', ν'') or (ν1',ν2',ν3') – (ν1'',ν2'',ν3'')
a	226.6	Al	226	$5d\ ^2D – 3p\ ^2P^o$	3/2 – 1/2; 5/2 – 3/2; 3/2 – 3/2
b	246.3	AlO	249	$D\ ^2\Sigma^+ – X\ ^2\Sigma^+$	(0,0)
c	257.5	Li	256	$5p\ ^2P^o – 2s\ ^2S$	3/2 – 1/2; 1/2 – 1/2
d	268.3	AlO	269	$D\ ^2\Sigma^+ – X\ ^2\Sigma^+$	(1,4)
e	290.5	Al AlO	291 289	$4d\ ^2D^o – 4d\ ^2D$ $C\ ^2\Pi – X\ ^2\Sigma^+$	5/2 – 5/2; 3/2 – 3/2 (3,1)
f	297.0	O	297	$2p^4\ ^1S – 2p^4\ ^3P$	0 – 1
g	319.8	Al	320	$4d\ ^2D^o – 6d\ ^2D$	5/2 – 5/2
h	341.0	Al Na	343 343	$3p^2\ ^4P – 3p\ ^2P^o$ $3d\ ^2D – 3s\ ^2S$; $3d\ ^4F^o – 3p(^3P^o)\ ^4S$	3/2 – 1/2 3/2 – 1/2; 5/2 – 3/2
i	348.8	Na	348	$3d\ ^4D^o – 3p(^3P^o)\ ^4S$	5/2 – 3/2
j	369.2	Li	371	$8d\ ^2D – 2p\ ^2P^o$	3/2 – 1/2; 5/2 – 3/2; 3/2 – 3/2
k	377.3	Li	379	$7d\ ^2D – 2p\ ^2P^o$	3/2 – 1/2; 5/2 – 3/2; 3/2 – 3/2
l	398.3	Al	396	$4s\ ^2S – 3p\ ^2P^o$	1/2 – 3/2
m	401.9	Na Na	399 400	$3d\ ^4P^o – 3p(^3P^o)\ ^4D$ $3d\ ^4P^o – 3p(^3P^o)\ ^4D$	3/2 – 3/2 1/2 – 3/2
n	404.6	K	404	$5p\ ^2P^o – 4s\ ^2S$	3/2 – 1/2; 1/2 – 1/2
o	451.4	AlO	451	$B\ ^2\Sigma^+ – X\ ^2\Sigma^+$	(3,1)
p	470.0	AlO	467	$B\ ^2\Sigma^+ – X\ ^2\Sigma^+$	(1,0)
q	485.9	AlO I	485 486	$B\ ^2\Sigma^+ – X\ ^2\Sigma^+$ $7p\ ^2[3]^o – 6s\ ^2[2]$	(0,0) 7/2 – 5/2
r	495.3	I K	491 496	$7p\ ^2[2]^o – 6s\ ^2[2]$ $8d\ ^2D – 4p\ ^2P^o$	5/2 – 5/2 5/2 – 3/2

s	503.7	Na	507	4s $^4P^o$ – 3p($^3P^o$) ^4D	7/2 – 5/2
t	527.4	Na	525	4s $^4P^o$ – 3p($^3P^o$) ^4D	5/2 – 3/2
u	533.4	I_2	532	B $^3\Pi_{0+u}$ – X $^1\Sigma_g^+$	(32,0)
v	539.6	AlO	538	B $^2\Sigma^+$ – X $^2\Sigma^+$	(1,3)
w	545.6	I I_2	542 545	6p $^2[1]^o$ – 6s $^2[2]$ B $^3\Pi_{0+u}$ – X $^1\Sigma_g^+$	3/2 – 5/2 (25,0)
x	559.2	O	557	2p^4 ^{1}S – 2p^4 ^{1}D	0–2
y	580.0	I_2	578	B $^3\Pi_{0+u}$ – X $^1\Sigma_g^+$	(16,1)
z	594.6	I_2	592	B $^3\Pi_{0+u}$ – X $^1\Sigma_g^+$	(14,2)
a	605.1	I_2	604	B $^3\Pi_{0+u}$ – X $^1\Sigma_g^+$	(13,3)
b	624.3	I_2	623	B $^3\Pi_{0+u}$ – X $^1\Sigma_g^+$	(10,4)
c	641.5	I_2 O	641 645	B $^3\Pi_{0+u}$ – X $^1\Sigma_g^+$ 5s $^5S^o$ – 3p ^5P	(8,5) 2–1; 2–2; 2–3
d	652.9	I_2	654	B $^3\Pi_{0+u}$ – X $^1\Sigma_g^+$	(7,6)
e	659.5	O	660	5s $^1D^o$ – 3p ^1F	2–3
f	674.6	H_2O Li	632-683 670	ro-vib. mode 2p $^2P^o$ – 2s ^2S	(1,1,3) – (1,5,1) 3/2 – 1/2; 1/2 – 1/2

Table S5: Peak assignments for the deconvoluted emission spectrum of AlH particle levitated in 60% O_2 and 40% Ar

Peak/band	Peak wavelength/band center (nm)	Carrier	Reference wavelength (nm)[22,23,24]	Transition	Branch; spin-orbit components; vibrational quantum numbers: (ν', ν'') or (ν1',ν2',ν3') – (ν1'',ν2'',ν3'')
a	215.4	Al	215	8d ^{2}D – 3p ^{2}P^o	5/2 – 3/2; 3/2 – 3/2
b	282.6	AlO	282	D $^2\Sigma^+$ – X $^2\Sigma^+$	(0,5)
c	295.9	AlO	296	C $^2\Pi$ – X $^2\Sigma^+$	(1,0)
d	360.5	Li	361	4s ^{4}P^o – 2p^2 ^{4}P	5/2 – 5/2; 3/2 – 5/2; 5/2 – 3/2; 3/2 – 3/2; 1/2 – 3/2; 3/2 – 1/2; 1/2 – 1/2
e	369.6	Li	367	9d ^{2}D – 2p ^{2}P^o	3/2 – 1/2; 3/2 – 3/2; 5/2 – 3/2
f	381.0	Li	379	7d ^{2}D – 2p ^{2}P^o	3/2 – 1/2; 5/2 – 3/2; 3/2 – 3/2
g	406.4	K	404	5p ^{2}P^o – 4s ^{2}S	3/2 – 1/2; 1/2 – 1/2
h	420.2	Na	418	3d ^{4}D^o – 3p(^{3}P^o) ^{4}P	5/2 – 5/2
i	440.0	IO	440	A $^2\Pi_{3/2}$ – X $^2\Pi_{3/2}$	(2,1)
j	479.5	I	476	7p ^{2}[1]^o – 6s ^{2}[2]	3/2 – 5/2
k	494.1	I K	491 496	7p ^{2}[2]^o – 6s ^{2}[2] 8d ^{2}D – 4p ^{2}P^o	5/2 – 5/2 5/2 – 3/2
l	513.9	Na	516	4s ^{4}P^o – 3p(^{3}P^o) ^{4}D	5/2 – 5/2
m	522.2	I	523	7p ^{2}[3]^o – 6s ^{2}[2]	5/2 – 3/2
n	530.2	I_2	532	B $^3\Pi_{0+u}$ – X $^1\Sigma_g^+$	(32,0)
o	534.9	AlO	538	B $^2\Sigma^+$ – X $^2\Sigma^+$	(1,3)
p	540.3	I I_2	542 545	6p ^{2}[1]^o – 6s ^{2}[2] B $^3\Pi_{0+u}$ – X $^1\Sigma_g^+$	3/2 – 5/2 (25,0)
q	544.8	IO	550	A $^2\Pi_{3/2}$ – X $^2\Pi_{3/2}$	(2,5)
r	569.9	AlO	565	B $^2\Sigma^+$ – X $^2\Sigma^+$	(2,5)
s	584.7	I_2	585	B $^3\Pi_{0+u}$ – X $^1\Sigma_g^+$	(16,2)
t	600.8	I_2	600	B $^3\Pi_{0+u}$ – X $^1\Sigma_g^+$	(12,2)
u	613.0	I_2	615	B $^3\Pi_{0+u}$ – X $^1\Sigma_g^+$	(10,3)

		O I_2	615 611	4d $^5D^o$ – 3p ^5P B $^3\Pi_{0+u}$ – X $^1\Sigma_g^+$	1–1; 3–2; 4–3 (11,3)
v	618.9	I_2	619	B $^3\Pi_{0+u}$ – X $^1\Sigma_g^+$	(9,3)
w	626.6	I_2	628	B $^3\Pi_{0+u}$ – X $^1\Sigma_g^+$	(9,4)
x	636.0	I_2	636	B $^3\Pi_{0+u}$ – X $^1\Sigma_g^+$	(7,4)
y	642.3	I_2	641	B $^3\Pi_{0+u}$ – X $^1\Sigma_g^+$	(8,5)
z	646.0	O	645	5s $^5S^o$ – 3p ^5P	2–1; 2–2; 2–3
a	661.7	O	660	5s $^1D^o$ – 3p ^1F	2–3
b	677.1	H_2O	632-683	ro-vib. mode	(1,1,3) – (1,5,1)
c	690.3	H_2O K	690-710 693	ro-vib. mode 4d ^2D – 4p $^2P^o$; 6s ^2S – 4p $^2P^o$	(1,0,3) – (0,0,0) 3/2 – 1/2; 1/2 – 3/2

Table S6: Peak assignments for the deconvoluted emission spectrum of AlH particle levitated in 70% O_2 and 30% Ar

Peak/band	Peak wavelength/band center (nm)	Carrier	Reference wavelength (nm)[22,23,24]	Transition	Branch; spin-orbit components; vibrational quantum numbers: (ν', ν'') or (ν1',ν2',ν3') – (ν1'',ν2'',ν3'')
a	235.5	AlO	235	$D\ ^2\Sigma^+ - X\ ^2\Sigma^+$	(3,0)
b	267.3	AlO	269	$D\ ^2\Sigma^+ - X\ ^2\Sigma^+$	(1,4)
c	369.9	Li	371	$8d\ ^2D - 2p\ ^2P^o$	3/2 – 1/2; 5/2 – 3/2; 3/2 – 3/2
d	400.0	Na Na	399 400	$3d\ ^4P^o - 3p(^3P^o)\ ^4D$ $3d\ ^4P^o - 3p(^3P^o)\ ^4D$	3/2 – 3/2 1/2 – 3/2
e	416.8	Na	418	$3d\ ^4D^o - 3p(^3P^o)\ ^4P$	5/2 – 5/2
f	426.7	Na Al	425 425	$3d\ ^4D^o - 3p(^3P^o)\ ^4P$ $3d\ ^2D^o - 5d\ ^2D$	5/2 – 3/2 5/2 – 5/2
g	489.4	I	486	$7p\ ^2[3]^o - 6s\ ^2[2]$	7/2 – 5/2
h	499.5	K	496	$8d\ ^2D - 4p\ ^2P^o$	5/2 – 3/2
i	510.5	AlO I	510 511	$B\ ^2\Sigma^+ - X\ ^2\Sigma^+$ $7p\ ^2[1]^o - 6s\ ^2[2]$	(0,1) 3/2 – 3/2
j	521.1	I	523	$7p\ ^2[3]^o - 6s\ ^2[2]$	5/2 – 3/2
k	529.4	Na	525	$4s\ ^4P^o - 3p(^3P^o)\ ^4D$	5/2 – 3/2
l	543.3	I I_2	542 545	$6p\ ^2[1]^o - 6s\ ^2[2]$ $B\ ^3\Pi_{0+u} - X\ ^1\Sigma_g^+$	3/2 – 5/2 (25,0)
m	557.4	Na Al	556 555	$4s\ ^4P^o - 3p(^3P^o)\ ^4P$ $6p\ ^2P^o - 4s\ ^2S$	3/2 – 3/2 3/2 – 1/2; 1/2 – 1/2
n	572.1	I_2	574	$B\ ^3\Pi_{0+u} - X\ ^1\Sigma_g^+$	(17,1)
o	583.6	I_2	585	$B\ ^3\Pi_{0+u} - X\ ^1\Sigma_g^+$	(16,2)
p	600.8	I_2	600	$B\ ^3\Pi_{0+u} - X\ ^1\Sigma_g^+$	(12,2)
q	626.4	I_2	623	$B\ ^3\Pi_{0+u} - X\ ^1\Sigma_g^+$	(10,4)
r	663.3	O I_2	660	$5s\ ^1D^o - 3p\ ^1F$ $B\ ^3\Pi_{0+u} - X\ ^1\Sigma_g^+$	2–3 (5,6)

			664		
s	674.0	H_2O Li	632-683 670	ro-vib. mode $2p\ ^2P^o - 2s\ ^2S$	(1,1,3) – (1,5,1) 3/2 – 1/2; 1/2 – 1/2
t	679.0	H_2O	632-683	ro-vib. mode	(1,1,3) – (1,5,1)
u	696.3	H_2O	690-710	ro-vib. mode	(1,0,3) – (0,0,0)

Table S7: Peak assignments for the deconvoluted emission spectrum of AlH particle levitated in 80% O_2 and 20% Ar

Peak/band	Peak wavelength/band center (nm)	Carrier	Reference wavelength (nm)[22,23,24]	Transition	Branch; spin-orbit components; vibrational quantum numbers: (ν', ν'') or (ν1',ν2',ν3') – (ν1'',ν2'',ν3'')
a	204.7	I	206	$6s\ ^2[2] – 5p^5\ ^2P^o$	3/2 – 1/2
b	215.9	Al	215	$8d\ ^2D – 3p\ ^2P^o$	5/2 – 3/2; 3/2 – 3/2
c	243.4	Li	242	$7p\ ^2P^o – 2s\ ^2S$	3/2 – 1/2; 1/2 – 1/2
d	258.6	AlO	255	$D\ ^2\Sigma^+ – X\ ^2\Sigma^+$	(0,1)
e	261.9	AlO	262	$D\ ^2\Sigma^+ – X\ ^2\Sigma^+$	(0,2)
f	265.7	AlO	269	$D\ ^2\Sigma^+ – X\ ^2\Sigma^+$	(1,4)
g	278.9	AlO	275	$D\ ^2\Sigma^+ – X\ ^2\Sigma^+$	(1,5)
h	295.7	AlO O	296 297	$C\ ^2\Pi – X\ ^2\Sigma^+$ $2p^4\ ^1S – 2p^4\ ^3P$	(1,0) 0 – 1
i	321.8	AlO	322	$C\ ^2\Pi – X\ ^2\Sigma^+$	(1,3)
j	335.5	AlO	340	$C\ ^2\Pi – X\ ^2\Sigma^+$	(0,4)
k	354.8	Na	350 351	$3d\ ^4P^o – 3p(^3P^o)\ ^4S$	3/2 – 3/2; 1/2 – 3/2
l	377.0	Li	379	$7d\ ^2D – 2p\ ^2P^o$	3/2 – 1/2; 5/2 – 3/2; 3/2 – 3/2
m	386.2	Na Na	384 386	$3d\ ^4F^o – 3p(^3P^o)\ ^4D$ $3d\ ^4F^o – 3p(^3P^o)\ ^4D$	5/2 – 5/2 7/2 – 7/2
n	392.8	Al O	394 394	$4s\ ^2S – 3p\ ^2P^o$ $4p\ ^5P – 3s\ ^5S^o$	1/2 – 1/2 3–2; 2–2; 1–2
o	402.1	Na Na	399 400	$3d\ ^4P^o – 3p(^3P^o)\ ^4D$ $3d\ ^4P^o – 3p(^3P^o)\ ^4D$	3/2 – 3/2 1/2 – 3/2
p	406.9	K	404	$5p\ ^2P^o – 4s\ ^2S$	3/2 – 1/2; 1/2 – 1/2
q	428.3	Na Al	425 425	$3d\ ^4D^o – 3p(^3P^o)\ ^4P$ $3d\ ^2D^o – 5d\ ^2D$	5/2 – 3/2 5/2 – 5/2
r	439.0	IO	440	$A\ ^2\Pi_{3/2} – X\ ^2\Pi_{3/2}$	(2,1)
s	453.3	AlO	451	$B\ ^2\Sigma^+ – X\ ^2\Sigma^+$	(3,1)
t	461.1	Li	460	$4d\ ^2D – 2p\ ^2P^o$	3/2 – 1/2; 5/2 – 3/2; 3/2 – 3/2
u	469.2	AlO	467	$B\ ^2\Sigma^+ – X\ ^2\Sigma^+$	(1,0)

v	499.3	K	496	8d ^{2}D – 4p ^{2}P^o	5/2 – 3/2
w	503.2	Na	507	4s ^{4}P^o – 3p(^{3}P^o) ^{4}D	7/2 – 5/2
x	523.9	I	523	7p ^{2}[3]^o – 6s ^{2}[2]	5/2 – 3/2
y	537.9	AlO	538	B $^2\Sigma^+$ – X $^2\Sigma^+$	(1,3)
z	543.6	I I_2	542 545	6p ^{2}[1]^o – 6s ^{2}[2] B $^3\Pi_{0+u}$ – X $^1\Sigma_g^+$	3/2 – 5/2 (25,0)
a	548.2	IO	550	A $^2\Pi_{3/2}$ – X $^2\Pi_{3/2}$	(2,5)
b	555.6	Na Al	556 555	4s ^{4}P^o – 3p(^{3}P^o) ^{4}P 6p ^{2}P^o – 4s ^{2}S	3/2 – 3/2 3/2 – 1/2; 1/2 – 1/2
c	565.1	AlO	565	B $^2\Sigma^+$ – X $^2\Sigma^+$	(2,5)
d	575.3	I_2	574	B $^3\Pi_{0+u}$ – X $^1\Sigma_g^+$	(17,1)
e	583.9	I_2	585	B $^3\Pi_{0+u}$ – X $^1\Sigma_g^+$	(16,2)
f	590.6	I_2 Na	592 589	B $^3\Pi_{0+u}$ – X $^1\Sigma_g^+$ 3p ^{2}P^o – 3s ^{2}S	(14,2) 1/2 – 1/2
g	601.4	I_2	600	B $^3\Pi_{0+u}$ – X $^1\Sigma_g^+$	(12,2)
h	607.2	I_2	604	B $^3\Pi_{0+u}$ – X $^1\Sigma_g^+$	(13,3)
i	610.9	I_2 Li	611 610	B $^3\Pi_{0+u}$ – X $^1\Sigma_g^+$ 3d ^{2}D – 2p ^{2}P^o	(11,3) 3/2 – 1/2; 5/2 – 3/2; 3/2 – 3/2
j	618.8	I_2 O	615 615	B $^3\Pi_{0+u}$ – X $^1\Sigma_g^+$ 4d ^{5}D^o – 3p ^{5}P	(10,3) 1–1; 3–2; 4–3
k	631.5	I_2	628	B $^3\Pi_{0+u}$ – X $^1\Sigma_g^+$	(9,4)
l	672.6	H_2O Li	632-683 670	ro-vib. mode 2p ^{2}P^o – 2s ^{2}S	(1,1,3) – (1,5,1) 3/2 – 1/2; 1/2 – 1/2
m	676.3	H_2O	632-683	ro-vib. mode	(1,1,3) – (1,5,1)
n	679.6	H_2O	632-683	ro-vib. mode	(1,1,3) – (1,5,1)

Table S8. Number of peaks in each species that are unique assignments with no overlapping assignments. Bolded species are the species with the most unique assignments. Non-bolded species are tentatively assigned. Dashes represent that the species is not detected at all and zeros represent the species that are assigned but have conflicting assignments with other species.

Species	10%	20%	30%	40%	50%	60%	70%	80%
I	2	3	3	2	0	2	2	2
AlO DX	-	4	1	2	2	1	2	4
AlO CX	0	3	1	1	0	1	-	2
Li	1	2	1	3	3	3	1	3
Al	0	0	1	1	3	1	0	1
OH	-	0	0	1	-	-	-	-
Na	3	9	1	5	4	2	3	4
O	0	3	1	0	3	2	0	0
K	2	3	1	3	1	1	1	2
IO	1	2	2	1	-	2	-	2
AlO BX	2	4	3	2	3	2	0	4
I_2	4	8	7	8	6	7	4	5
H_2O	-	2	1	2	0	1	2	2

Table S9: Peak assignments for the deconvoluted emission spectrum of AID particle levitated in 20% O_2 and 80% Ar

Peak/band	Peak wavelength/band center (nm)	Carrier	Reference wavelength (nm)[22,23,24,27]	Transition	Branch; spin-orbit components; vibrational quantum numbers: (ν', ν'') or (ν1',ν2',ν3') – (ν1'',ν2'',ν3'')
a	205.7	I	206	$6s\ ^2[2] – 5p^5\ ^2P^o$	3/2 – 1/2
b	234.6	AlO	235	$D\ ^2\Sigma^+ – X\ ^2\Sigma^+$	(3,0)
c	240.7	Li	242	$7p\ ^2P^o – 2s\ ^2S$	3/2 – 1/2; 1/2 – 1/2
d	253.5	AlO	255	$D\ ^2\Sigma^+ – X\ ^2\Sigma^+$	(0,1)
e	257.2	Li	256	$5p\ ^2P^o – 2s\ ^2S$	3/2 – 1/2; 1/2 – 1/2
f	264.3	OD	263	$A\ ^2\Sigma^+ – X\ ^2\Pi$	(3,1)
g	282.6	AlO	282	$D\ ^2\Sigma^+ – X\ ^2\Sigma^+$	(0,5)
h	286.6	OH Na	287 – 289 285	$A\ ^2\Sigma^+ – X\ ^2\Pi$ $5p\ ^2P^o – 3s\ ^2S$	R_1, R_2, Q_1, Q_2; (2, 1) 3/2 – 1/2; 1/2 – 1/2
i	289.7	Al AlO OD	291 289 289	$4d\ ^2D^o – 4d\ ^2D$ $C\ ^2\Pi – X\ ^2\Sigma^+$ $A\ ^2\Sigma^+ – X\ ^2\Pi$	5/2 – 5/2; 3/2 – 3/2 (3,1) (1,0)
j	294.6	OD	296 297	$A\ ^2\Sigma^+ – X\ ^2\Pi$ $A\ ^2\Sigma^+ – X\ ^2\Pi$	(3,2) (2,0)
k	316.8	AlO	313	$C\ ^2\Pi – X\ ^2\Sigma^+$	(0,1)
l	321.2	Al	320	$4d\ ^2D^o – 6d\ ^2D$	5/2 – 5/2
m	324.5	AlO	322	$C\ ^2\Pi – X\ ^2\Sigma^+$	(1,3)
n	329.1	Na	330	$4p\ ^2P^o – 3s\ ^2S$	3/2 – 1/2; 1/2 – 1/2
o	348.1	Na	348	$3d\ ^4D^o – 3p(^3P^o)\ ^4S$	5/2 – 3/2
p	364.9	K Li	364 367	$4d\ ^2D – 4s\ ^2S$ $9d\ ^2D – 2p\ ^2P^o$	3/2 – 1/2; 5/2 – 1/2 3/2 – 1/2; 3/2 – 3/2; 5/2 – 3/2
q	370.6	Li	371	$8d\ ^2D – 2p\ ^2P^o$	3/2 – 1/2; 5/2 – 3/2; 3/2 – 3/2
r	412.3	I	410	$6p\ ^2[3]^o – 6s\ ^2[2]$	7/2 – 5/2
s	464.0	AlO	467	$B\ ^2\Sigma^+ – X\ ^2\Sigma^+$	(1,0)
t	478.2	I	476	$7p\ ^2[1]^o – 6s\ ^2[2]$	3/2 – 5/2
u	495.3	I K	491 496	$7p\ ^2[2]^o – 6s\ ^2[2]$ $8d\ ^2D – 4p\ ^2P^o$	5/2 – 5/2 5/2 – 3/2

v	505.5	Na	507	4s $^4P^o$ – 3p($^3P^o$) ^4D	7/2 – 5/2
w	511.7	AlO I	510 511	B $^2\Sigma^+$– X $^2\Sigma^+$ 7p $^2[1]^o$ – 6s $^2[2]$	(0,1) 3/2 – 3/2
x	523.9	I	523	7p $^2[3]^o$ – 6s $^2[2]$	5/2 – 3/2
y	529.8	I_2	532	B $^3\Pi_{0+u}$ – X $^1\Sigma_g^+$	(32,0)
z	534.8	AlO	538	B $^2\Sigma^+$– X $^2\Sigma^+$	(1,3)
a	545.6	IO	550	A $^2\Pi_{3/2}$ – X $^2\Pi_{3/2}$	(2,5)
b	556.9	Na Al	556 555	4s $^4P^o$ – 3p($^3P^o$) ^4P 6p $^2P^o$ – 4s ^2S	3/2 – 3/2 3/2 – 1/2; 1/2 – 1/2
c	568.8	AlO	565	B $^2\Sigma^+$– X $^2\Sigma^+$	(2,5)
d	583.6	I_2	585	B $^3\Pi_{0+u}$ – X $^1\Sigma_g^+$	(16,2)
e	590.8	I_2 Na	592 589	B $^3\Pi_{0+u}$ – X $^1\Sigma_g^+$ 3p $^2P^o$ – 3s ^2S	(14,2) 1/2 – 1/2
f	599.3	I_2	600	B $^3\Pi_{0+u}$ – X $^1\Sigma_g^+$	(12,2)
g	607.7	I_2	604	B $^3\Pi_{0+u}$ – X $^1\Sigma_g^+$	(13,3)
h	620.1	I_2	619	B $^3\Pi_{0+u}$ – X $^1\Sigma_g^+$	(9,3)
i	628.4	I_2 I_2	628 632	B $^3\Pi_{0+u}$ – X $^1\Sigma_g^+$ B $^3\Pi_{0+u}$ – X $^1\Sigma_g^+$	(9,4) (8,4)
j	635.9	I_2	636	B $^3\Pi_{0+u}$ – X $^1\Sigma_g^+$	(7,4)
k	651.5	I_2	649	B $^3\Pi_{0+u}$ – X $^1\Sigma_g^+$	(8,6)
l	662.4	O	660	5s $^1D^o$ – 3p ^1F	2–3
m	665.6	I_2	664	B $^3\Pi_{0+u}$ – X $^1\Sigma_g^+$	(5,6)
n	671.3	H_2O Li	632-683 670	ro-vib. mode 2p $^2P^o$ – 2s ^2S	(1,1,3) – (1,5,1) 3/2 – 1/2; 1/2 – 1/2
o	685.1	H_2O	632-683	ro-vib. mode	(1,1,3) – (1,5,1)

Data S1: Basefunctions of various temperature dependent transitions extracted from PGOPHER showing A) AlO BX transition, B) AlO CX transition, C) AlO DX transition, D) IO, E) I_2

References

[1] G.L. Rizzo, S. Biswas, I. Antonov, K.K. Miller, M.L. Pantoya, R.I. Kaiser, Exotic Inverse Kinetic Isotopic Effect in the Thermal Decomposition of Levitated Aluminum Iodate Hexahydrate Particles. *J. Phys. Chem. Lett.* **2023**, *14*, 2722–2730.